A POTENTIAL TECHNIQUE TO DETERMINE THE UNSATURATED SOIL SHEAR STRENGTH PARAMETER

A Thesis

by

RENU UDAY KULKARNI

Submitted to the Office of Graduate Studies of
Texas A&M University
in partial fulfillment of the requirements for the degree of

MASTER OF SCIENCE

August 2008

Major Subject: Civil Engineering

A POTENTIAL TECHNIQUE TO DETERMINE THE UNSATURATED SOIL SHEAR STRENGTH PARAMETER

A Thesis

by

RENU UDAY KULKARNI

Submitted to the Office of Graduate Studies of
Texas A&M University
in partial fulfillment of the requirements for the degree of

MASTER OF SCIENCE

Approved by:

Chair of Committee,	Jean-Louis Briaud
Committee Members,	Giovanna Biscontin
	Frederick Chester
Head of Department,	David Rosowsky

August 2008

Major Subject: Civil Engineering

ABSTRACT

A Potential Technique to Determine the Unsaturated Soil Shear Strength Parameter.

(August 2008)

Renu Uday Kulkarni,

B.E., University of Mumbai, Mumbai, India

Chair of Advisory Committee: Dr. Jean-Louis Briaud

The shear strength behavior of unsaturated soils is a complex phenomenon. The major factors that lead to the complex behavior are grain size, natural alteration in status of moisture and associated capillary potential. The need for research is felt to understand the various aspects associated with development of shear strength of unsaturated soils.

The research is conducted to obtain the most economical and reliable design solutions. The magnitude of positive pore water pressure developed in saturated soil reduces the shear strength to a great extent. The tensile pore water pressure in the capillary meniscus developed around the soil grain contacts, on the contrary, enhances the factor of safety in the case of unsaturated soil mass. In this research, the shear strength of unsaturated soil is studied for a range of saturation based on the parametric study.

The principle of effective stress has proven to be the basis for understanding the shear strength of saturated soil mass and it has provided an explanation for the geotechnical engineering problems.

The thesis presents a study on the shear strength of the soil specimen using the direct shear apparatus. The previous research was mainly directed towards evaluation of shear strength under controlled soil suction, by modifying the apparatus. A simple technique is put forward in this research by making use of the conventional direct shear apparatus for testing the unsaturated soil. The suction stress was induced in the soil specimen and the shear strength was evaluated. The soil water characteristic curve has been used in the research to determine the tensile pore water pressure. Hypothesis based on parametric study has been put forward to present a technique to determine the unsaturated soil shear strength parameter in the thesis.

To my parents

ACKNOWLEDGEMENTS

My heartiest gratitude goes to Dr. Jean-Louis Briaud for his support, guidance and patience throughout this research. I also acknowledge the contribution of Dr. Giovanna Biscontin and Dr. Frederick Chester for their valuable guidance in preparing this document.

I thank the Civil Engineering Department for providing financial support during my graduate studies at Texas A&M University. I thank Mr. Mike Linger for providing testing equipment at the Civil Lab. I also acknowledge the help offered by Remon Abdelmalak, Hamid Reza Nouri and Lumani Sigdel during laboratory testing. I thank all my friends for their encouragement to finish the research.

Special thanks to my parents, Dr. Uday Kulkarni and Mrs. Rashmi Kulkarni, for their unconditional love, prayers and encouragement.

TABLE OF CONTENTS

Page

CHAPTER Page

CHAPTER Page

LIST OF FIGURES

FIGURE Page

FIGURE Page

FIGURE Page

LIST OF TABLES

CHAPTER I

INTRODUCTION

Shear strength has great significance in geotechnical engineering with design applications in slope stability analysis, retaining wall design, design of foundations and many such noteworthy instances. The potential geotechnical engineering solutions are dictated by shear strength of the soil. The solutions derived by considering 100% degree of saturation, are fairly conservative to establish realistic and economical solutions. Fredlund (2006) has mentioned the significance of unsaturated soil mechanics in engineering practice. Hence, the unsaturated shear strength equation plays an important role in the analyses.

The major applications for this equation are summarized below:

1. To establish factor of safety for the existing slopes.
2. To design the deep cuts to accommodate raft foundations and to ensure their stability.
3. To establish safe bearing capacity for temporary/enabling constructions like scaffolding in non-monsoon periods.
4. For soils subjected to alternate wetting and drying.
5. To carry out the retaining wall design.
6. To run slope stability analyses.
7. To evaluate safe bearing capacity of the soil for the foundation design.

The principle of effective stress developed by Terzaghi in 1936 has widely formed the basis for understanding shear strength of saturated soils. However to understand the engineering features of unsaturated soils, this theory needs to be modified. Geotechnical engineering is a discipline where the engineering properties are measured and not specified.

This thesis follows the style of the *ASCE Journal of Geotechnical and Geoenvironmental Engineering.*

A hypothesis is presented to determine the unsaturated shear strength parameter and is experimentally validated. The main objective of this study is to determine the relationship between the unsaturated soil shear strength parameter and the degree of saturation using the clay specimen.

The following plan is used in the thesis:

1. The effective stress equation advocated by Briaud et al. (2007) has been used as the basis to predict the parameter.
2. Bishop et al. (1960) established the effective stress principle for the unsaturated soil in terms of unsaturated shear strength parameter χ. A significant amount of research has been done to study this equation. A discussion of this has been presented in literature review (Chapter II). An understanding of the equation developed by Fredlund et al. (1995) has also been presented in the same chapter.
3. Chapter III presents the engineering properties of the soil.
4. The salt equilibrium test was carried out on the specimens by inducing osmotic suction. Chapter IV presents a discussion on the soil water characteristic curve which is used as a tool in the research to determine the tensile pore water pressure.
5. The shear strength is determined using the conventional direct shear test apparatus. The procedure adopted for measuring the shear strength for saturated and unsaturated soil is discussed in chapter V.
6. Chapter VI explains the research methodology adopted during the study. The data is presented and analyzed in Chapter VII. The overall conclusions from the study, the recommendations and the scope for future work are discussed in Chapter VIII.

1.1 Fundamentals

The shear strength of the soil is defined as the maximum stress the soil can resist just before the failure. Soils are seldom subjected to direct shear. They are generally subjected to direct compression as they are particulate materials. Soil failure in shear occurs when the applied compressive loads exceed the shear strength of the soil. The

types of stress that exist on the soil at a point, the principle of effective stress and the failure envelope for the saturated soils are described next.

1.1.1 State of stress on a plane

The stress on the plane at a specific point has two stress components:

1. Normal stress (σ) – it acts normal to the plane and compresses the soil grains towards each other. This is responsible for the volume change.
2. Shear Stress (τ) – it acts on the plane tangentially and slides the soil grains relative to each other. This leads to rotation and ultimate failure of the soil.

Figure 1.1 explains the phenomenon.

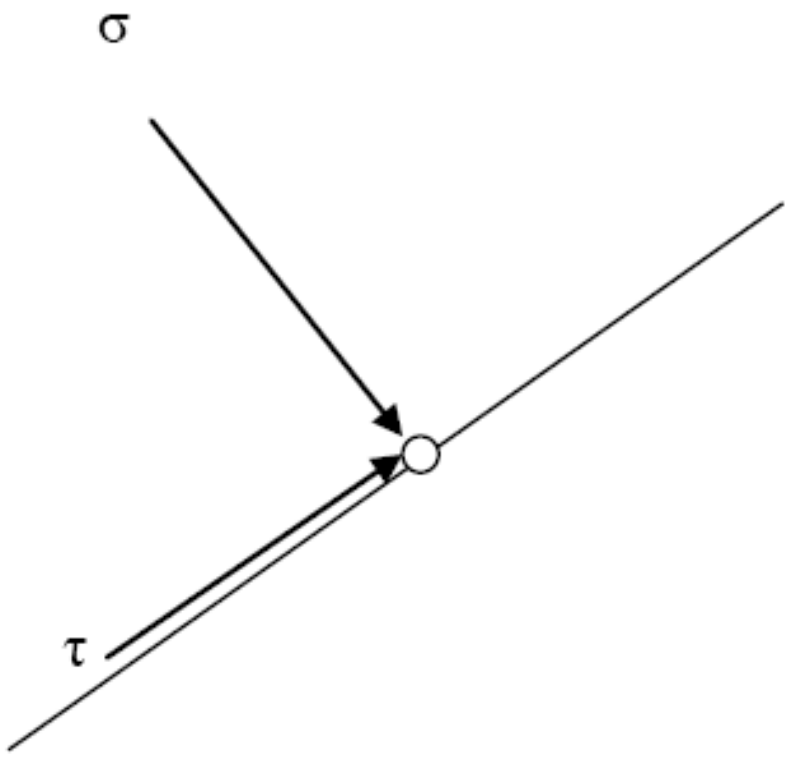

Fig. 1.1 The stress components

1.1.2 Effective stress principle

The effective stress principle using the one state variable for the saturated soils developed by Terzaghi (1936) is formulated as:

$$\sigma' = \sigma - u_w \quad (1)$$

where,

σ' = effective stress on the failure plane

σ = total vertical stress on the soil

u_w = positive pore water pressure exerted on the soil

Edil (2005) has discussed the equation elaborately.

Total vertical stress exerted on a plane is:

$$\sigma = \sum\gamma\, \Delta z + q \quad (2)$$

where,

$\sum\gamma\, \Delta z$ = geostatic stress due to weight of soil layers above the point where γ is the unit weight of the soil and Δz is the layer thickness

q = change in the vertical load (plus or minus) due to the surface loads.

Figure 1.2 shows the total vertical stress acting on the soil element under consideration.

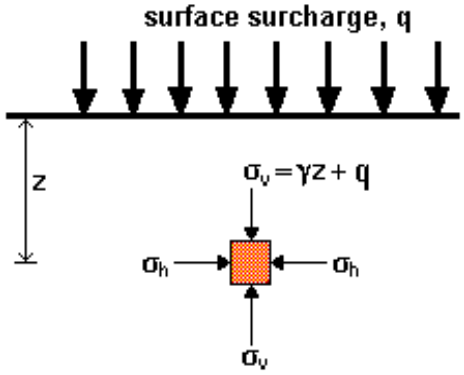

Fig. 1.2 Total vertical stress (Atkinson 2000)

Pore water pressure exerted on the soil is:

$$u_w = u_0 + \Delta u_e \quad (3)$$

where,

$u_0 = h_p \gamma_w$, water pressure due to static or flowing ground water, where, h_p = pressure head and γ_w is the unit weight of water

Δu_e = pore pressure change resulting from stress changes (cut or fill, erosion, etc.) and is a function of shear and normal stress changes, degree of saturation, stress history, etc.

Figure 1.3 shows the pore water pressure exerted in the soil mass under hydrostatic conditions.

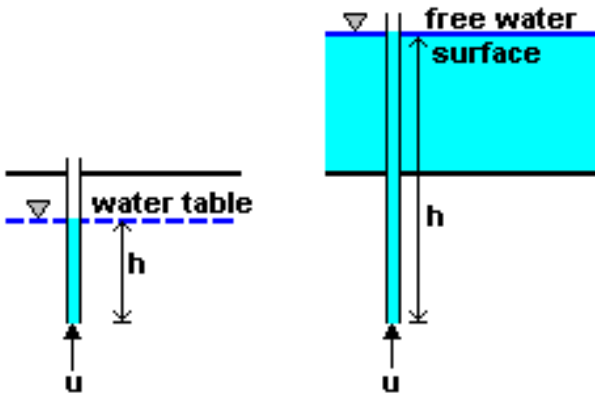

Fig. 1.3 Pore water pressure (Atkinson 2000)

The effective stress is the force transmitted at the contacts divided by the total area. It is obtained by subtracting the neutral stress from the total stress. Figure 1.4 shows the effective stress generated in the soil mass.

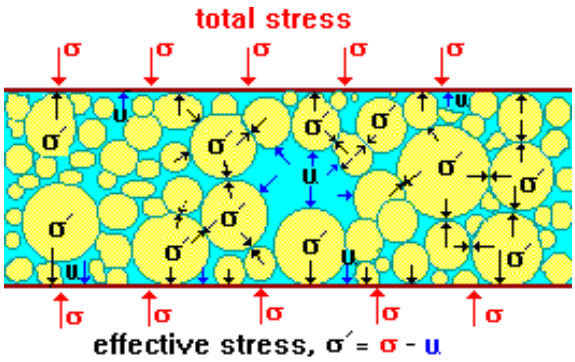

Fig. 1.4 Effective stress (Atkinson 2000)

The pore water pressure is also called the neutral stress since it does not have shear component. And from the fluid mechanics principles we have the pore water pressure to be equal in magnitude in all directions. The total and effective stress can be resolved into normal and shear components.

1.2 Failure

The failure in soil is due to direct shear. The failure criterion of the soil adopted in this study, the failure envelope for the normally consolidated drained test for the saturated samples and the failure envelope for the unsaturated soil samples are discussed next.

1.2.1 Mohr-Coulomb failure criterion

The Mohr-Coulomb failure criterion can be explained in terms of the effective stress. The failure is defined by the linear envelope. The following figure shows the failure of the soil specimen. The shear stress at failure and the normal stress when plotted on the graph for shear stress τ vs. σ', shear strength parameters, c' and Φ' can be obtained. Figure 1.5 shows the failure of the sample by triaxial testing and the failure envelope obtained after the test.

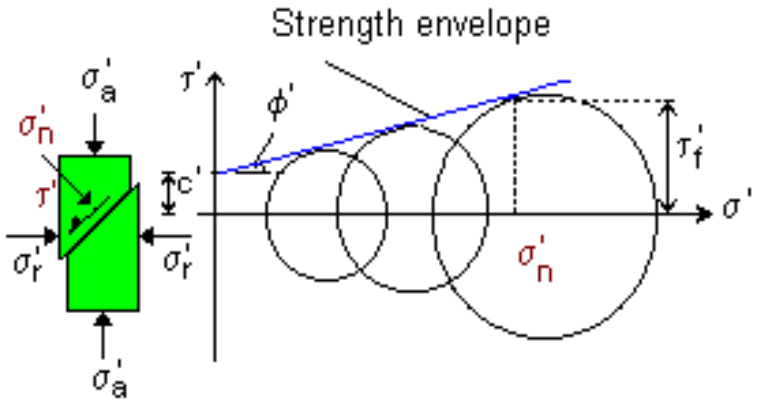

Fig. 1.5 Failure envelope (Atkinson 2000)

1.2.2 Failure envelope for normally consolidated clay in drained condition

The failure envelope for the saturated specimen is obtained according to Mohr-Coulomb equation for the drained test. The shear strength parameters c' and Φ' are determined from this envelope. A typical Mohr failure envelope for the normally consolidated clay in drained shear could be represented as in figure 1.6.

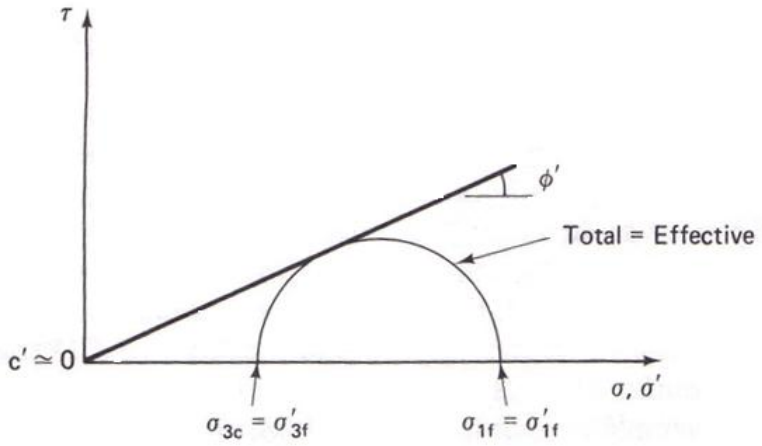

Fig. 1.6 Failure envelope for normally consolidated clay in drained condition (Holtz and Kovacs 1981)

1.2.3 Failure envelope for unsaturated soil sample

The failure envelope for unsaturated soil is non-linear as seen in figure 1.7.

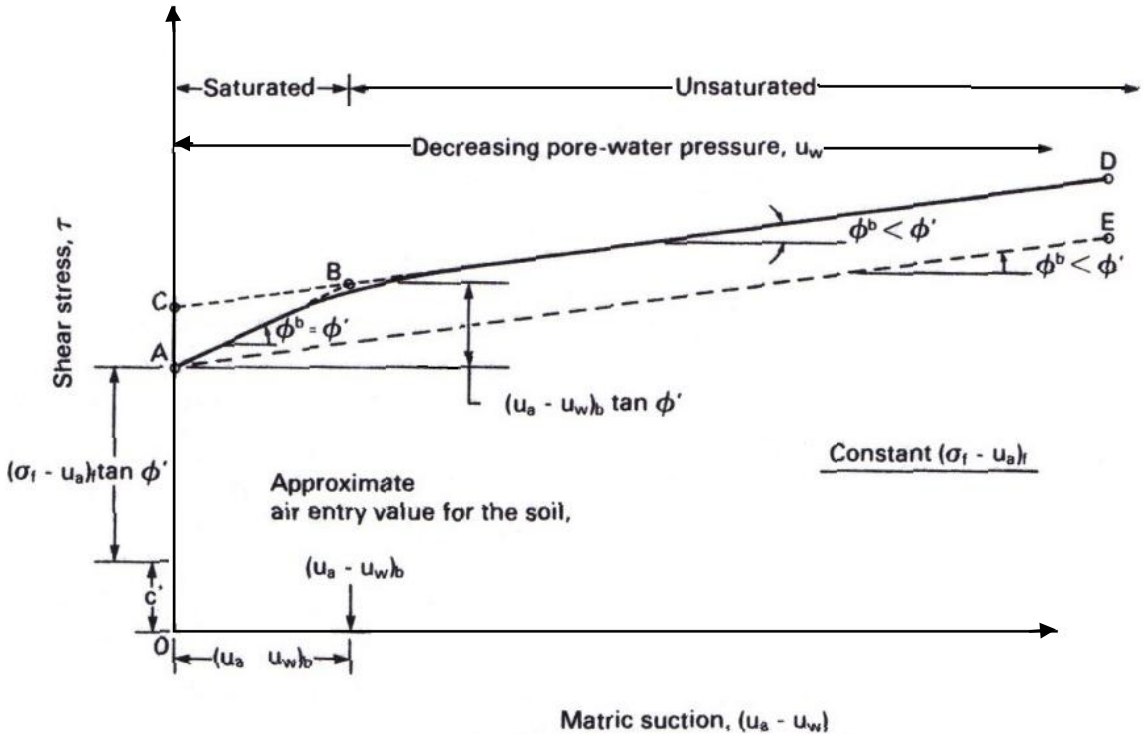

Fig. 1.7 Failure envelope for unsaturated soil (Fredlund and Rahardjo 1993)

Terzaghi presented the equation for the shear strength of the soil in terms of effective stress which is given as:

$$s = c' + \sigma' \tan \Phi'$$

where,

s = shear strength of specimen

c' = cohesion intercept

σ' = effective stress of the specimen on the failure plane

Φ' = effective friction angle

Shear stress is given as:

$$\tau = \frac{F}{A}$$

where,

F = shear force (N)

A = initial area of the sample (mm^2)

Normal stress acting on the specimen,

$$\sigma = \frac{N}{A}$$

where,

N = normal vertical force acting on the specimen (N)

A = initial area of the sample (mm^2)

1.3 Major zones according to saturation

Soil is believed to be saturated below the ground water level (zone 3) as can be seen in figure 1.8. It is saturated above the GWL by the chemical action between silica and water up to a certain height (zone 2). This is known as capillary zone. Above this zone the soil gets dried and hence unsaturated due to the heat of the sun (zone 1). Tensile pore water pressure, u_w is exerted in this zone.

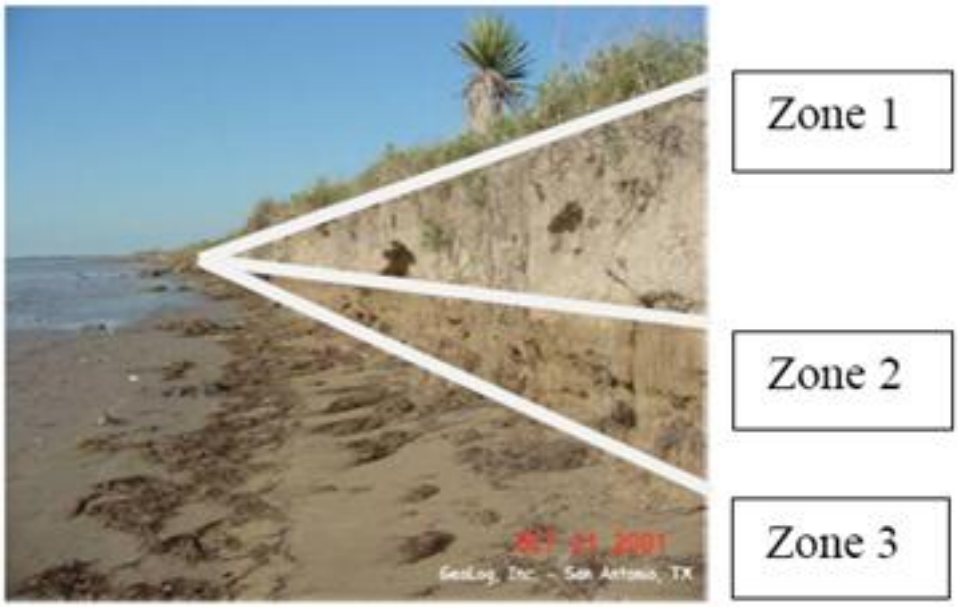

Fig. 1.8 Three zones indicating the state of soil redrawn (Briaud et al. 2007)

Briaud et al. (2007) stated that the principle of effective stress is valid only for degree of saturation ranging from 85% to 100%. The distinction is understood for the different states of the soil formed due to the different degree of saturation. Figure 1.9 shows the three different states of the soil. The first case in figure1.9 is when $S_r = 100\%$, the second case is when $S_r = 85\%$ and the third case is when $S_r < 85\%$. The effective stress equation for each of the three cases is given in table 1.1.

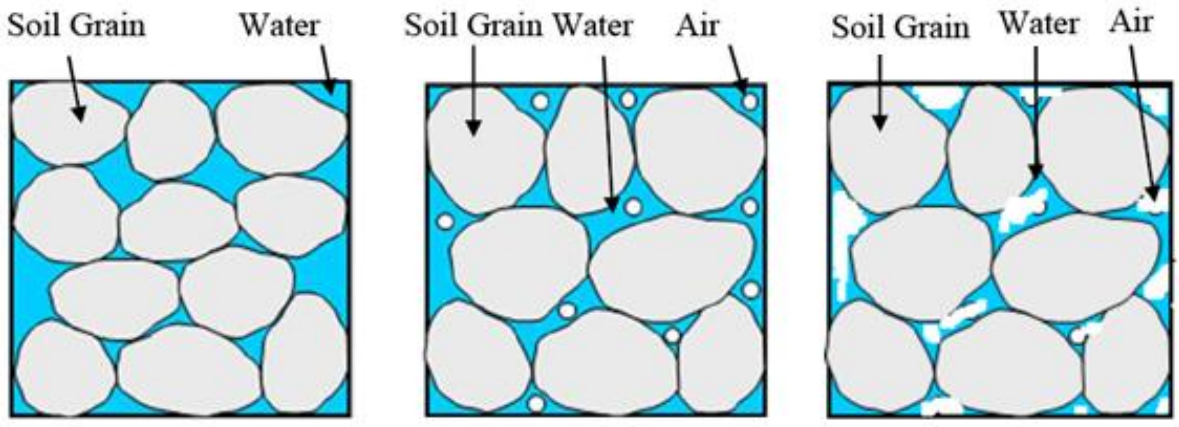

Fig. 1.9 Three states of soil saturation redrawn (Briaud et al. 2007)

Table 1.1 Effective stress for three states of soils (Briaud et al. 2007)

Case	**Degree of saturation**	**Pore pressure**	**Effective stress**
Saturated	100%	$u_w \neq 0$, $u_a = 0$	$\sigma' = \sigma - u_w$
Occluded air	85%	$u_w = u_a$	$\sigma' = \sigma - u_w$
Continuous air	<85%	$u_w \neq 0$, $u_a = 0$	$\sigma' = \sigma - \alpha * u_w$

Where,

$\alpha = \frac{A_w}{A_{Tot}}$ = unsaturated shear strength parameter.

1.4 Unsaturated effective stress equation derivation

The effective stress equation is derived in accordance with Briaud et al. (2007). Figure 1.10 shows the free body diagram of the unsaturated soil mass.

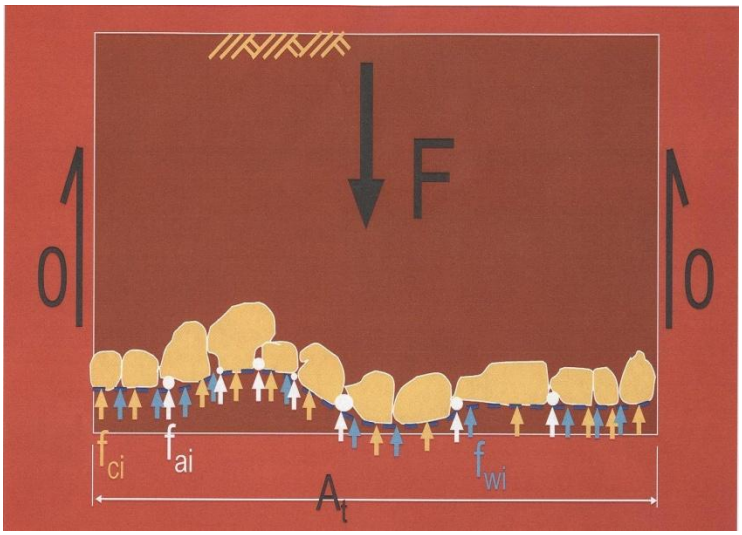

Fig. 1.10 Free body diagram of the soil showing equilibrium (Briaud et al. 2007)

The equilibrium on the wavy plane is discussed as follows:

$$F = \sum f_{ci} + \sum f_{wi} + \sum f_{ai} \quad (4)$$

$$F / A_t = \sum f_{ci} / A_t + \sum f_{wi} / A_t + \sum f_{ai} / A_t \quad (5)$$

where,

f_{ci} = force at the contact of soil grains.

f_{wi} = pressure exerted by pore water.

f_{ai} = pressure exerted by pore air.

A_t = total area on the wavy plane.

From figure 1.9, the following can be derived:

$$\sigma = \sigma' + \sum u_w * a_{wi} / A_t + \sum u_a * a_{ai} / A_t \quad (6)$$

$$\sigma = \sigma' + u_w . \sum a_{wi} / A_t + u_a . \sum a_{ai} / A_t \quad (7)$$

$$\alpha = \sum a_{wi} / A_t \qquad \beta = \sum a_{ai} / A_t \quad (8)$$

$$\sigma = \sigma' + \alpha * u_w + \beta * u_a \quad (9)$$

$$A_t = A_C + \sum a_{wi} + \sum a_{ai} \quad (10)$$

$$1 = A_c / A_t + \alpha + \beta \qquad A_c / A_t = 0 \quad (11)$$

$$\alpha + \beta = 1 \quad (12)$$

Thus, for the unsaturated case, the effective stress equation is given as:

$$\sigma' = \sigma - \alpha\, u_w - \beta\, u_a \quad (13)$$

where,

u_a = Tensile pore air pressure exerted on the soil

u_w = Tensile pore water pressure exerted on the soil

$$\beta = A_a/A_t \quad (14)$$

And for atmospheric air pressure, the above equation reduces to:

$$\sigma' = \sigma - \alpha\, u_w \quad (15)$$

1.5 Suction

At the contact points of soil grains, negative pore water pressure is exerted on the unsaturated soils. Likos and Lu (2002) have stated that the positive pore water pressure is responsible for pushing the soil grains away from each other, whereas the negative pore water pressure pulls the soil particles close to each other. The suction is measured with units of pF, kPa and cm rise of water.

The soil suction can be measured by the height h_c, in cm, to which a water column could be drawn by suction in a soil mass from external stress. The common logarithm of this height (cm) is known as the pF value. The relationship between the units for measuring is summarized as:

$10^{(pF-1)}$ = 1kPa

10^{pF} = Height of the meniscus in cm.

1.6 Shear strength

Shear strength is the maximum stress that can be applied tangentially on a plane within a soil mass before sliding occurs on that plane. Shear strength depends on the frictional resistance between the particles at their points of contact, cohesion between particles (if any exists), and the interlocking of particles within the soil skeleton. The failure in the soil occurs because of the relative movement of the particles (rolling and slipping of the grains) and not by breaking of them.

The Mohr-Coulomb failure criterion in terms of effective stress is expressed as:

$$s = c' + \sigma' \tan \Phi' \quad (16)$$

This is the equation of failure envelope.

where,

s = shear strength of the soil

c' = cohesion intercept

Φ' = angle of shearing resistance

σ' = effective stress

Some of the stress-strain relationships have been summarized in figure 1.11.

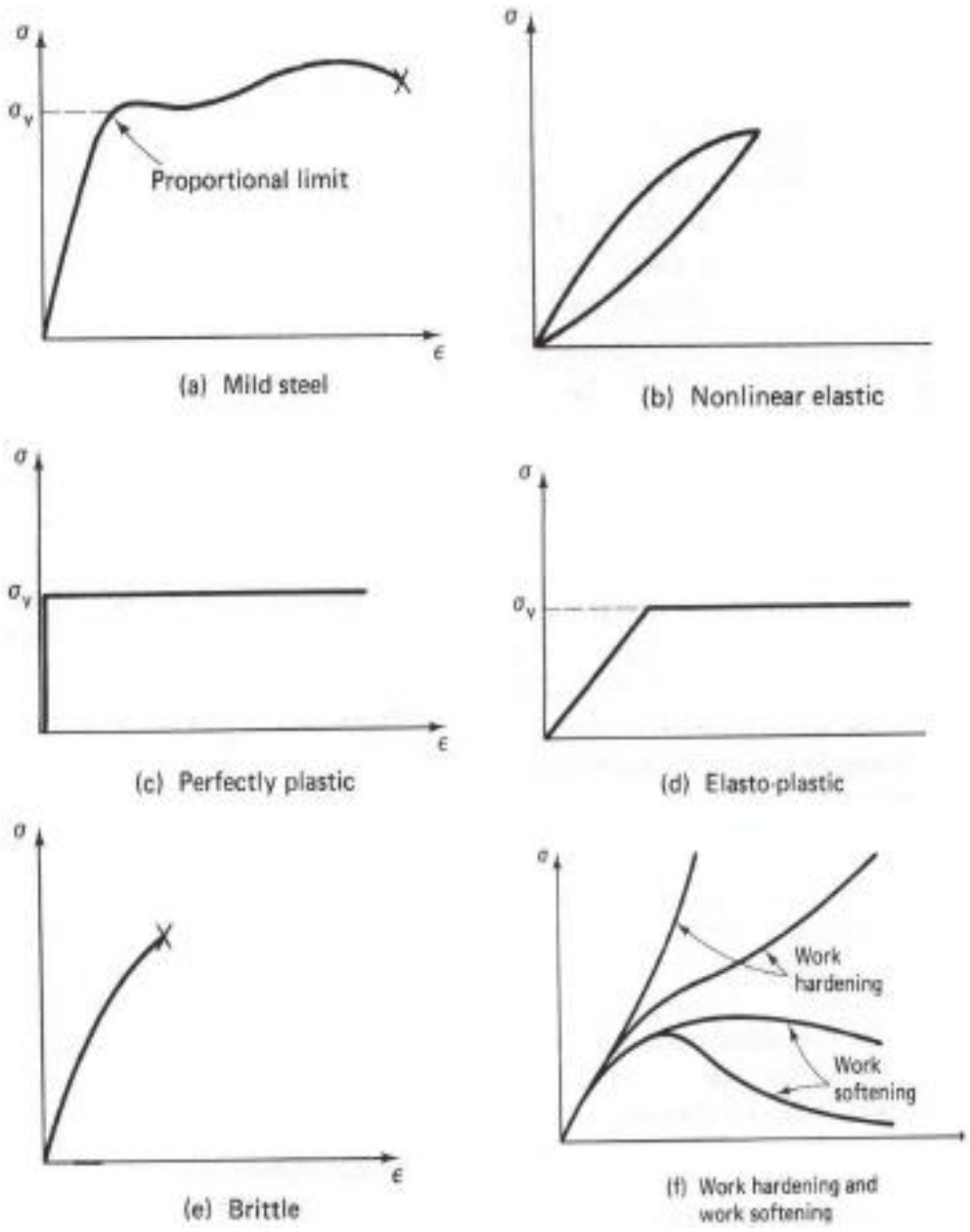

Fig. 1.11 Typical stress strain relationships for real and ideal materials (Holtz and Kovacs 1981)

1.7 Cohesion

The intercept on the plot for shear stress vs. effective stress is known as cohesion as seen in figure 1.5. Cohesion holds the particles of soil together in a soil mass and is independent of the normal stress.

1.8 Apparent cohesion

For a specific degree of saturation, under different normal loads, the failure envelope is obtained. The horizontal projection of this is obtained as seen in figure 1.12. The apparent cohesion is equal to the product of tensile pore water pressure and tangent of the friction angle.

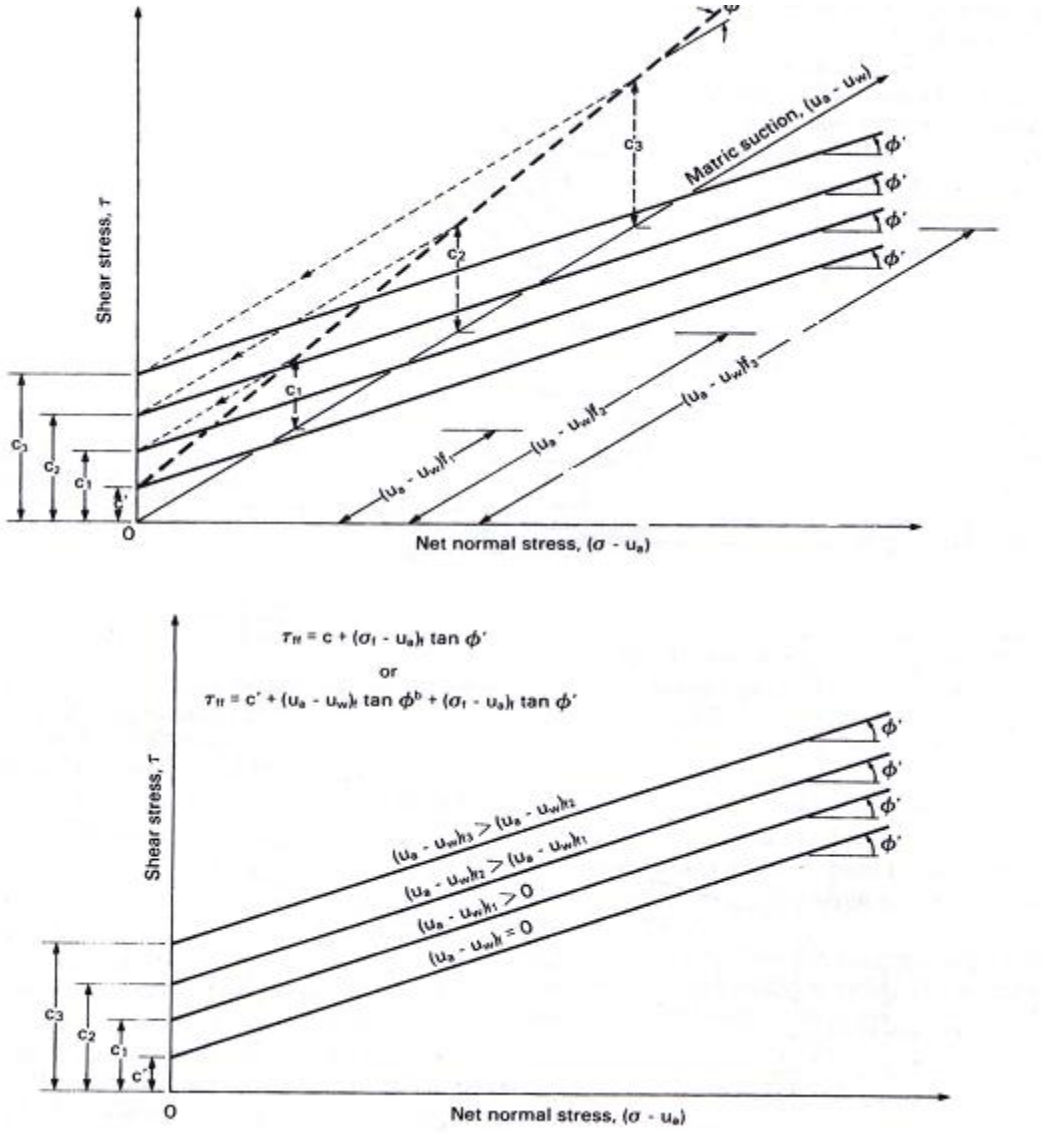

Fig. 1.12 Horizontal projection of the failure envelope for unsaturated soil (Fredlund and Rahardjo 1993)

1.9 Soil water characteristic curve (SWCC)

The soil water characteristic curve has been used as a tool in this research to define the tensile pore water pressure of the specimen for varying degrees of saturation. It is expressed as a plot for degree of saturation vs. suction or gravimetric (or volumetric) water content vs. suction. A detailed explanation on this curve is provided in Chapter III.

1.10 Types of SWCC-unimodal and bimodal curves

The curve with one bend is called unimodal and the one with two bends is called bimodal. This is explained by Gitirana and Fredlund (2004) as seen in figure 1.13.

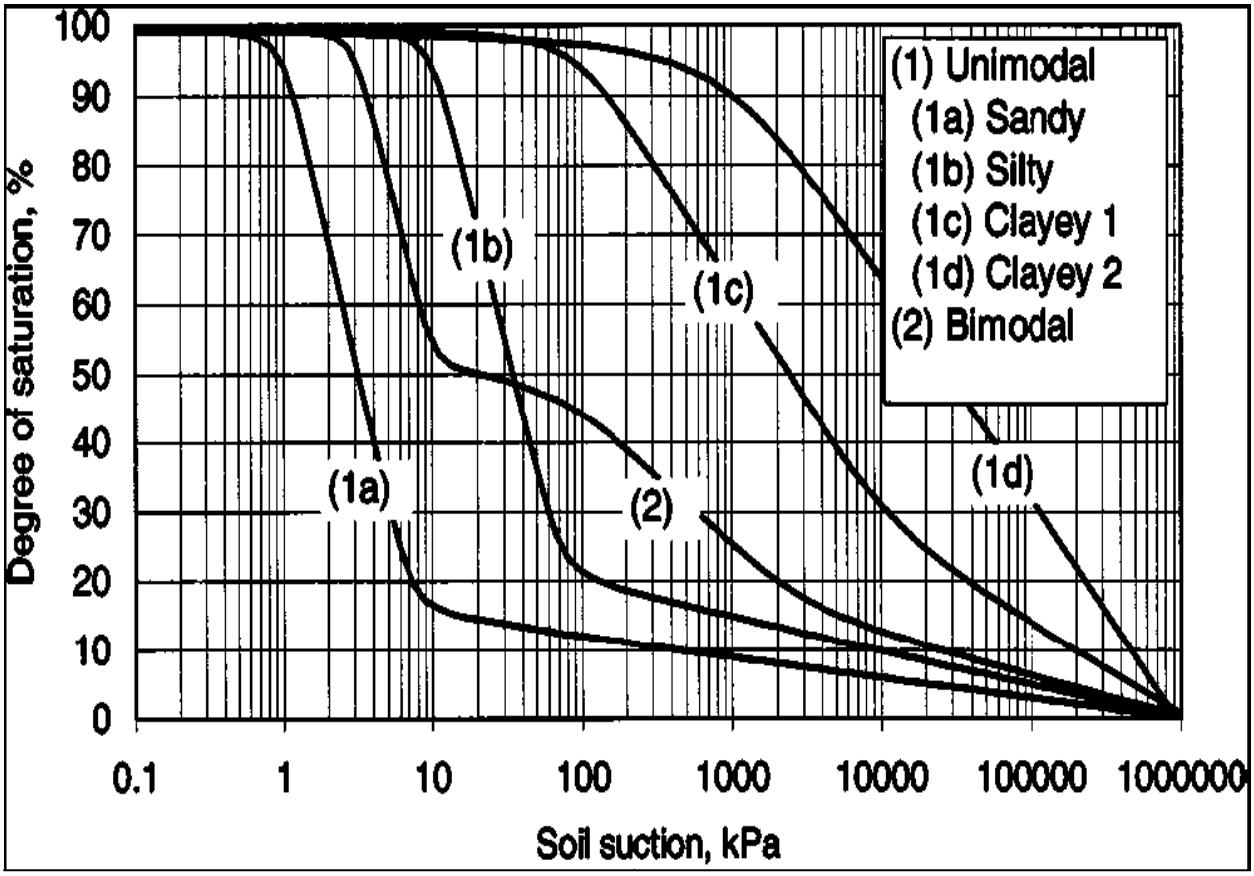

Fig. 1.13 SWCC conceptualizations (Gitirana and Fredlund 2004)

In this research, the unsaturated shear strength parameter α is predicted from the direct shear test under controlled laboratory conditions on the clay specimen. The tensile pore water pressure is measured by using SWCC in this study. Major conclusions are drawn from these tests and are validated by using the pertinent knowledge and results obtained from the tests.

CHAPTER II

LITERATURE REVIEW

Unsaturated soil shear strength is a complex phenomenon, due to the dominant role of the suction forces associated with such a soil system apart from the other factors. Explanation given here is pertinent to the present impressions about the various aspects related to shear strength determination.

This chapter presents a review on the previous research. The unsaturated shear strength equations developed by the various research workers will be discussed in this chapter. The literature review indicated that the direct shear test apparatus used for the study was modified. The details of the modified apparatus along with the rate of strain adopted by the previous researchers to shear the soil specimen will also be provided in this chapter. The various methods to measure the tensile pore water pressure will be analyzed. Finally, the work by the researchers to predict the χ parameter is presented.

2.1 Previous research

Significant research has been conducted to determine the unsaturated soil shear strength equation. The modified direct shear and triaxial apparatus have been widely used for this purpose.

Fredlund et al. (1978) put forward an equation by considering any two of the three state variables, $(\sigma - u_a)$, $(\sigma - u_w)$ and $(u_a - u_w)$ to define the shear strength for unsaturated soil which is given below.

$$\tau = c' + (\sigma - u_a) \tan \Phi' + (u_a - u_w) \tan \Phi^b \quad (17)$$

where,

Φ^b = friction angle depending upon the matric suction $(u_a - u_w)$.

Fredlund et al. (1978) later proposed that the soil should be treated as a four phase system with the air, water, soil solids and the contractile skin. It was also confirmed that the failure envelope was non-linear which is discussed in Chapter V.

As quoted by Fredlund et al. (1995) and attributed to Lamborn (1986), the shear strength equation developed using the principle of irreversible thermodynamics is:

$$\tau = c' + (\sigma - u_a) \tan \Phi' + (u_a - u_w)\, \theta_w \tan \Phi' \quad (18)$$

where,

θ_w is volumetric water content

Bishop and Eldin (1950) developed an equation for the effective stress which is stated below.

$$\sigma' = (\sigma - u_a) + \chi\, (u_a - u_w) \quad (19)$$

where,

χ = scaling factor that controls the value of tensile pore water pressure with values between 0 to 1

And the shear strength equation was given as:

$$\tau = c' + \sigma' \tan \Phi'$$

The values of c' and Φ' were determined at full saturation. Bishop et al. (1960) assumed that the values of c' and Φ' are independent of degree of saturation and that their values and volume change during shear may be influenced if there is a presence of air in the voids.

Bishop et al. (1960) observed that the rate of volume change at failure is found to vary with the degree of saturation even for the same stress history and this will influence the relevant value of Φ'. The corrected value of Φ' is used in the calculation of χ values. Bishop et al. (1960) stated that χ depends on the hysteresis effect i.e. the difference between wetting and drying.

The following major conclusions were drawn by Bishop et al. (1960):

1. It is necessary to use the modified equation for effective stress when the degree of saturation falls below 100%.
2. The use of more general expression $\sigma' = \sigma - u_a + \chi\ (u_a - u_w)$ takes into account both pore water and pore air pressure. The experiments indicate that χ depends on degree of saturation.

3. It is difficult to obtain the values of c' and Φ'. Hence, care should be taken while drawing the conclusions from laboratory tests.

Jennings and Burland (1962) stated that the principle of effective stress is not valid below a certain degree of saturation. They also proved that the effective stress equation provided by Bishop et al. (1960) does not provide an adequate relationship between void ratio and effective stress.

Four types of triaxial tests were run on the sample to determine the χ parameter by Bishop et al. (1960). The tests were conducted for:

1. Unconsolidated undrained
2. Constant water content
3. Consolidated undrained
4. Consolidated drained conditions

The tests were carried out as saturated drained tests with positive cell pressure and zero pore water pressure or as unsaturated drained tests in which a negative pore water pressure is applied. The amount of water draining from the sample and the overall volume change were measured to calculate the average degree of saturation of the sample. For the undrained condition, the pore water and pore air pressures were measured.

The soil samples chosen for the study were:

1. Braehead silt
2. London clay (LL = 66%, PL = 27%)
3. Compacted Boulder clay (Clay fraction 4%, OMC = 9.3%, Compaction water content 7.9%)
4. Clay shale

2.2 Apparatus for shear strength determination

Substantial research has been focused on predicting the value of the parameter χ. All tests were performed using modified triaxial or direct shear apparatus on saturated and

unsaturated soil samples. The technique used for inducing the soil suction and the modified apparatus is discussed next

2.2.1 Axis translation technique

Some of the researchers have used axis translation technique to induce tensile pore water pressure. In this external air pressure is applied on the sample. This leads to the generation of pore water pressure and thus the matric suction (u_a-u_w) is maintained constant. This technique requires the control of air pressure and measurement of water pressure.

2.2.2 Apparatus

Triaxial and direct shear tests apparatus have been widely used by various researchers to determine the shear strength of the soil sample. Herkal et al. (1995) observed certain difficulties while carrying out the drained and undrained test using the triaxial apparatus. It was observed that water entered the neighboring air pores when the drainage was closed. Also, when the soil sample was allowed to drain, water did not expel out before filling in the large air pores (S_r < 85 % - 90 %).

Escario and Saez (1987) developed a modified direct shear apparatus as shown in figure 2.1. Working principle was similar to that of the pressure membrane apparatus. Thus, relation between suction and water content, swelling and collapse of soil were all measured using this technique under controlled suction conditions.

The modifications were made in the apparatus to maintain the suction stress in the sample. The nitrogen was introduced under pressure in the upper part of the soil sample through a coarse grained porous stone. The lower face of the sample is in contact with water at atmospheric pressure through a high air entry value porous stone (15 kg/cm^2). Suitable time was allowed for the equilibrium. At this stage, the pore water pressure is equal to the applied air pressure. Push rods were used to monitor the vertical and lateral

force and displacements. The size of the sample used for the test was 22 mm in height. This small height of the sample allowed lesser time for equilibrium.

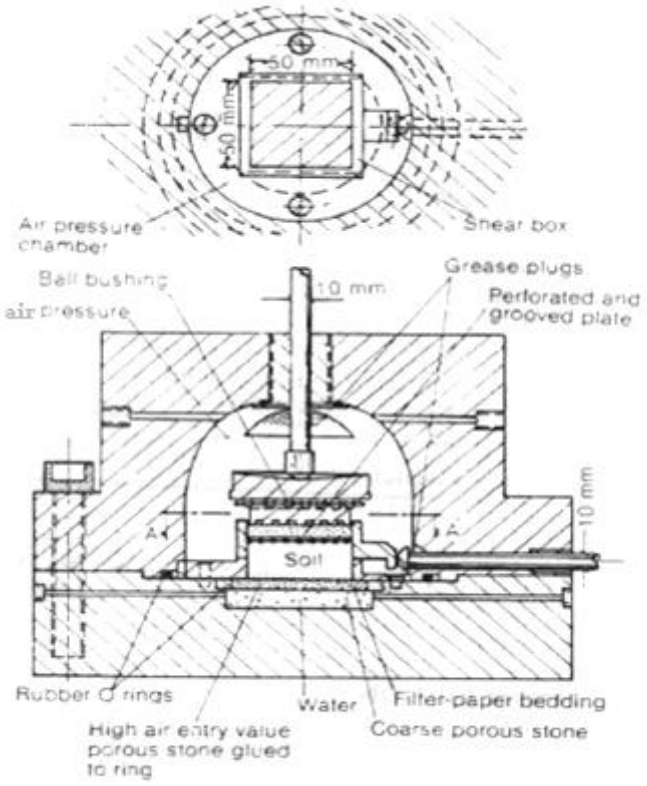

Fig. 2.1 The direct shear apparatus redrawn (Escario and Saez 1987)

Campos and Carillo (1995) also used a modified apparatus to measure the shear strength of the soil sample. The apparatus was similar to the one developed by Escario and Saez (1987) with one difference in the load monitoring. In this apparatus, an internal load cell was used to monitor vertical load transferred to the sample. To keep the vertical load being applied constant throughout the shearing phase, the load was transferred to the sample through the universal joint. The test apparatus and the apparatus layout is shown in figures 2.2 and 2.3 respectively. The test results obtained from this experiment are presented in figure 2.4.

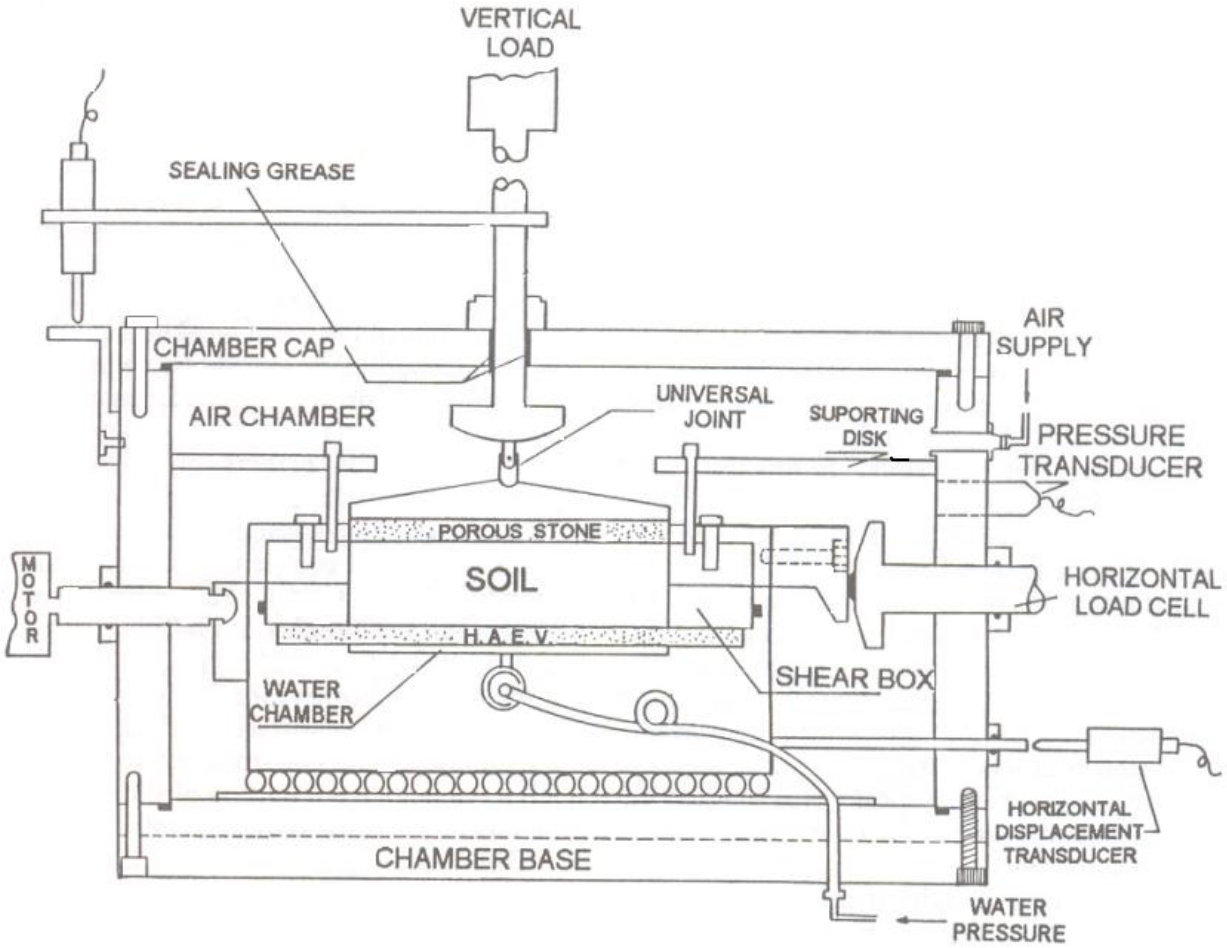

Fig. 2.2 Cross section of the new direct shear device (Campos and Carillo 1995)

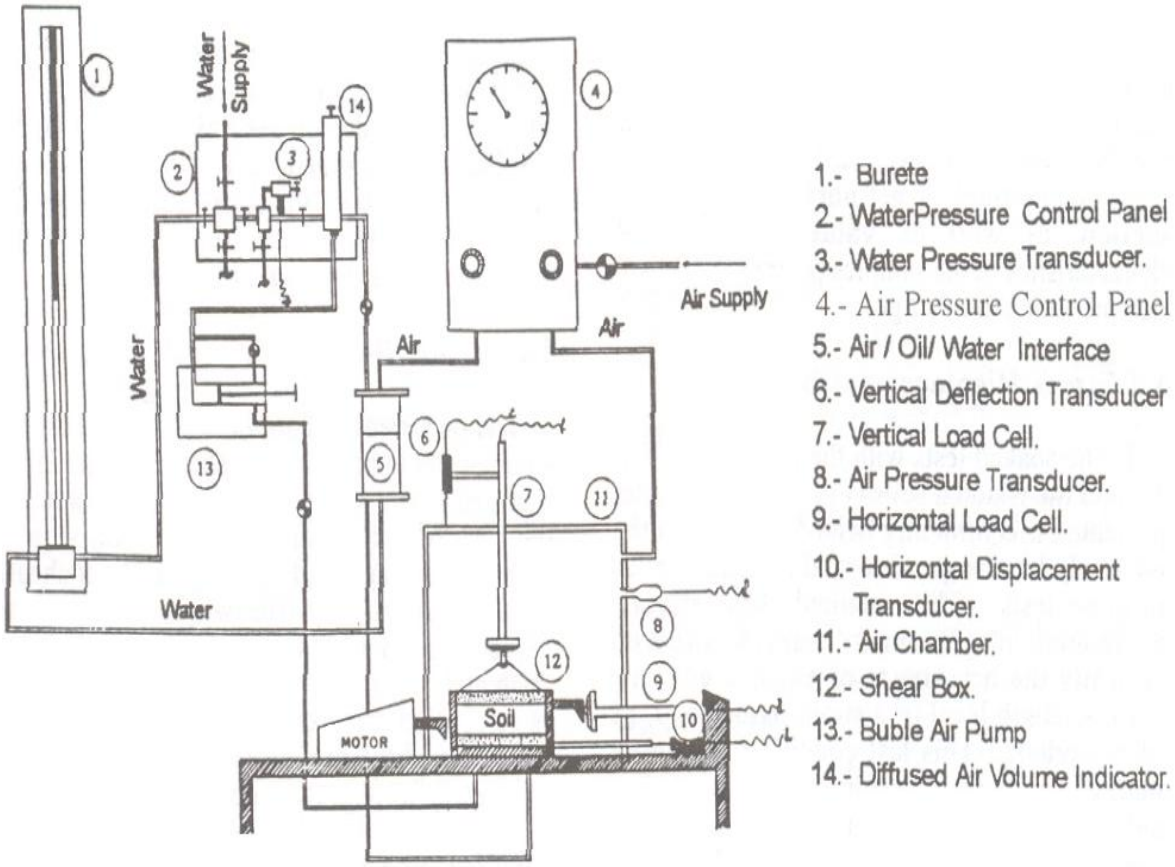

Fig. 2.3 Layout of the direct shear equipment set up (Campos and Carillo 1995)

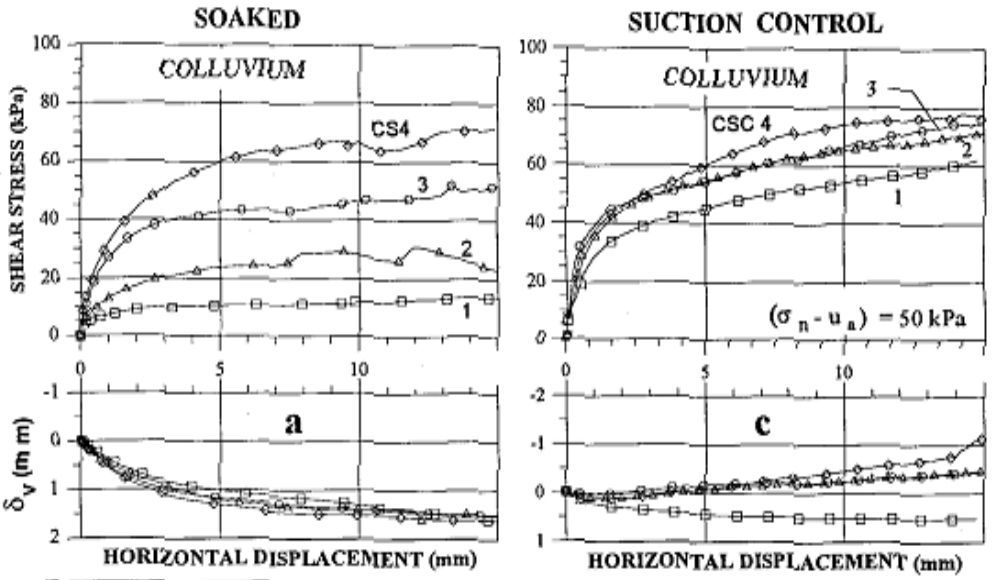

TEST	σ_n (kPa)	γ_{nat} kN/m³	w% initial	e initial	S initial
CS 1	20	13.44	11.59	1.3	25.59
CS 2	50	14.60	23.94	1.3	50.82
CS 3	90	15.54	24.11	1.2	57.12
CS 4	110	14.90	22.32	1.2	50.29

TEST	$u_a - u_w$ (kPa)	γ_{nat} kN/m³	w% initial	e initial	S initial
CSC 1	30	15.57	24.8	1.2	58.4
CSC 2	80	15.61	23.2	1.1	56.2
CSC 3	150	14.93	24.4	1.3	53.5
CSC 4	210	15.67	23.9	1.1	57.7

TEST	σ_n (kPa)	γ_{nat} kN /m³	w% initial	e initial	S initial
RS 1	20	15.82	20.5	1.1	53.1
RS 2	50	19.45	19.9	0.67	81.8
RS 3	90	16.98	15.0	0.84	49.6
RS 4	110	17.10	14.5	0.82	49.1

TEST	$u_a - u_w$ (kPa)	γ_{nat} kN/m³	w% initial	e initial	S initial
RSC 1	30	16.3	16.4	0.94	48.4
RSC 2	80	15.2	16.7	1.09	42.6
RSC 3	150	15.6	16.9	1.04	45.3
RSC 4	210	17.1	17.7	0.87	56.4

Fig. 2.4 Shear displacement curves obtained in the conventional and suction controlled tests (Campos and Carillo 1995)

2.3 Methods to measure the tensile pore water pressure

The methods to determine the tensile pore water pressure are enlisted in table 2.1. The choice of method is done on the grounds of time available, the range of suction values to be obtained and economy.

Table 2.1 Summarized information for the various methods available on soil suction determination (Ridley and Wray 1996)

Device	Measurement mode	Range (kPa)	Approximate equilibrium time
Thermocouple Psychrometer	Total	100 to 7500	Minutes
Thermisor/Transistor Psychrometer	Total	100 to 71000	Minutes
Filter paper(in-contact)	Matrix	30 to 30000	7 Days
Filter paper(no-contact)	Total	400 to 30000	7-14 Days
Porous block	Matrix	30 to 3000	Weeks
Thermal conductivity probe	Matrix	0 to 300	Weeks
Suction plate	Matrix	0 to -90	Hours
Pressure plate	Matrix	0 to 1500	Hours
Standard tensiometer	Matrix	0 to -100	Minutes
Osmotic tensiometer	Matrix	0 to 1500	Hours
IC tensiometer	Matrix	0 to -1800	Minutes

2.4 Soil water characteristic curve

The tensile pore water pressure is another important parameter in this study. SWCC is used to measure this value during the research. The SWCC depends on certain properties of soil like, soil texture, consolidation and compaction. This can be seen from the figure 2.5.

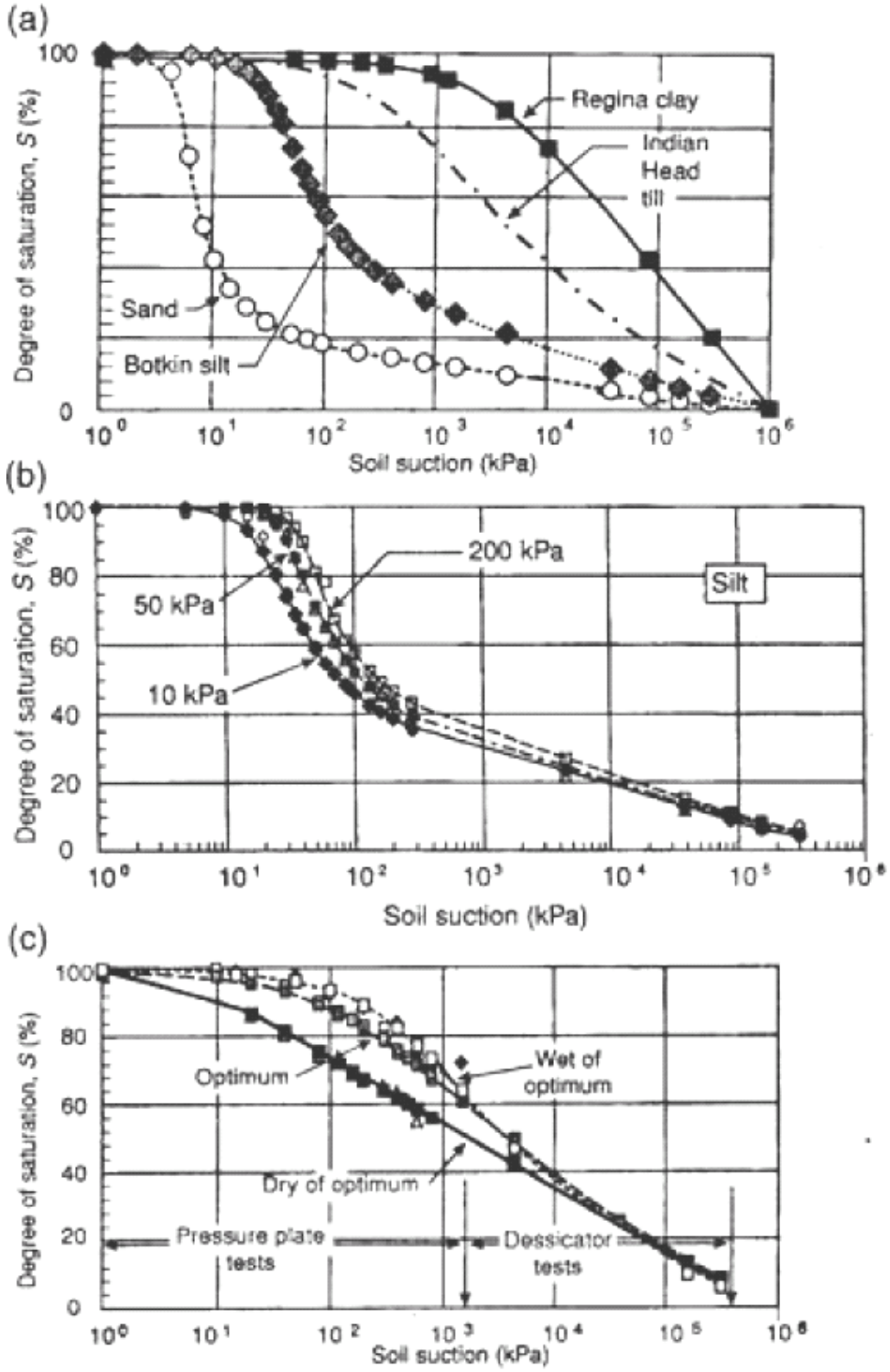

Fig. 2.5 Influence of soil texture, consolidation and compaction on the water retention properties of soils (Delage 2002)

2.5 Methods to obtain parameter χ

As quoted by Öberg and Sällfors (1995) and attributed to Croney et al. (1958), Aitchison (1960) and Jennings (1960) similar equations were proposed by considering soil as a three phase system consisting of air, water and soil solids. They used the gauge pressure which is referenced to the external air pressure. If the pore air pressure is used in the equation, their equations become identical to the equation presented by Bishop et al. (1960). In the literature review, it was found that the equation stated by Bishop et al. (1960) is adopted most commonly.

Aitchison (1960) formulated a theoretical equation for evaluating χ parameter.

$$\chi = \frac{\sigma'}{p''} = S_r + \frac{1}{p''}\sum_{0}^{p''} 0.3 p'' \Delta S_r$$

where,

p″ = pressure deficiency

= matric suction (u_a-u_w)

S_r = degree of saturation

Öberg and Sällfors (1995) quoted a relationship between χ and S_r, established by Donald (1961) using the theoretical equation proposed by Aitchison as seen in figure 2.6.

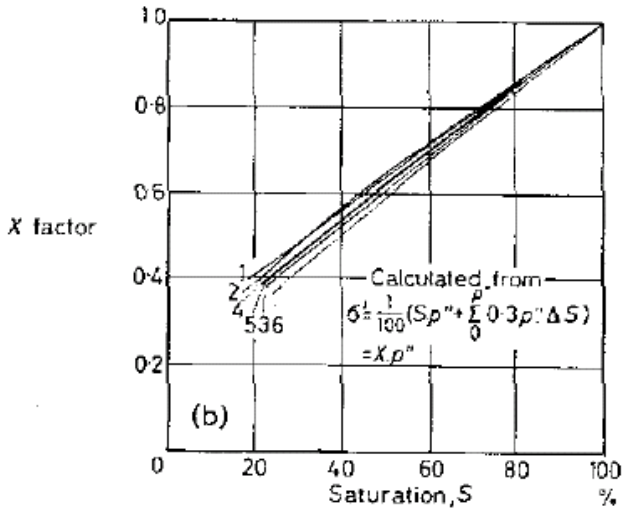

Fig. 2.6 Theoretical relation between χ and S_r (Öberg and Sällfors 1995)

Jennings and Burland (1962) performed a comparison study. The theoretical values for χ were compared with those obtained from the experiment by Bishop et al. (1960). It was observed that the experimental curve for the silty material, the χ vs. S_r was in accordance with the theoretical curve. This was particularly true for the degree of saturation ranging from 100% to 60-40%. For the clayey material, the curve departed from the theoretical curve. The test results obtained from the experiments is presented in figure 2.7.

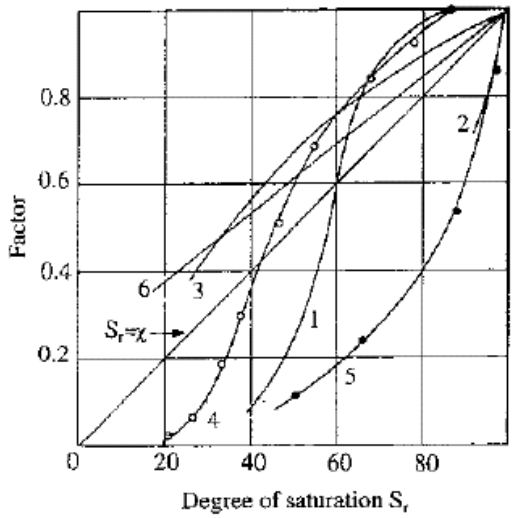

Where,

1. Compacted boulder clay (-2μ=4%), Bishop et al (1960)
2. Compacted shale (-2μ=22%), Bishop et al (1960)
3. Breahead silt, Bishop & Donald (1961)
4. Silt (-2μ=3%)
5. Silty clay (-2μ=23%)
6. Theoretical, Donald (1961)

Fig. 2.7 Plot for χ vs. S_r (Jennings and Burland 1962)

Escario and Juca (1989) conducted the direct shear tests using the modified apparatus developed by Escario and Juca (1989). The sample size was 50 mm x 50 mm and 22 mm in height. Table 2.2 describes the material and consolidation properties for

each of the soil samples. The soil water characteristic curve for these was obtained as seen in figure 2.8.

Table 2.2 Soil characteristics, initial conditions, consolidation time and rate of shear of samples tested (Escario and Juca 1989)

	Madrid grey clay 'Peneula'	**Red clay of Guadalix de la Sierra**	**Madrid clayey sand 'Arena de miga'**
Atterberg limits			
W_L	71	33	32
PI	35	13.6	15
Sieve analysis % passing			
10	–	–	100
16	–	100	94
40	100	97	48
200	99	86.5	17
Standard proctor test			
γ_{max} (g/cm^3)	1.33	1.80	1.91
W_{opt} (%)	33.7	17.0	11.5
Initial Conditions			
γ (g/cm^3)	1.33	1.80	1.91
W (%)	29	13.6	9.2
Suction (kg/cm^2)	8.5	2.8	0.7
Time of consolidation under surcharge and suction applied (days)	4	4	4
Rate of shear (mm/day)	2.4	2.4	2.4
Time to failure (days)	2.5–3	2–3	1–2

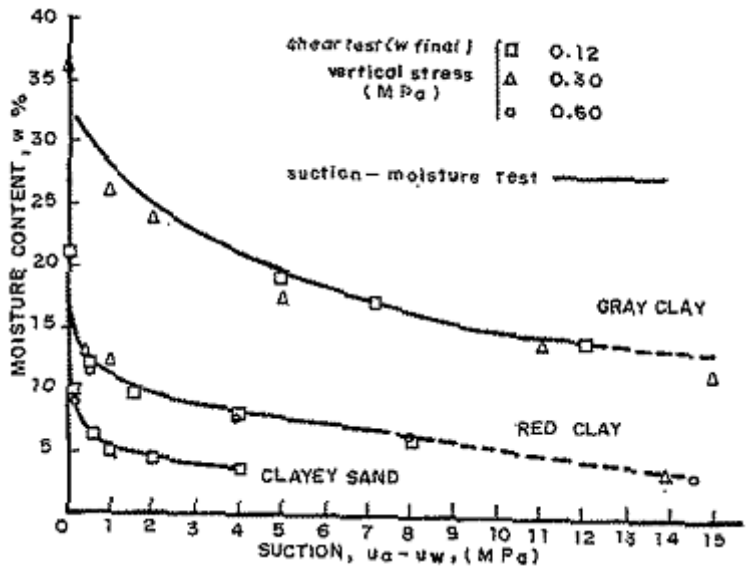

Fig. 2.8 Suction-moisture content relationships and final moisture content in the shear tests (Escario and Juca 1989)

The plot for shear stress vs. suction for Madrid grey clay, Red clay and Madrid clayey sand with the best curve fit is are presented in figure 2.9, 2.10 and 2.11 respectively.

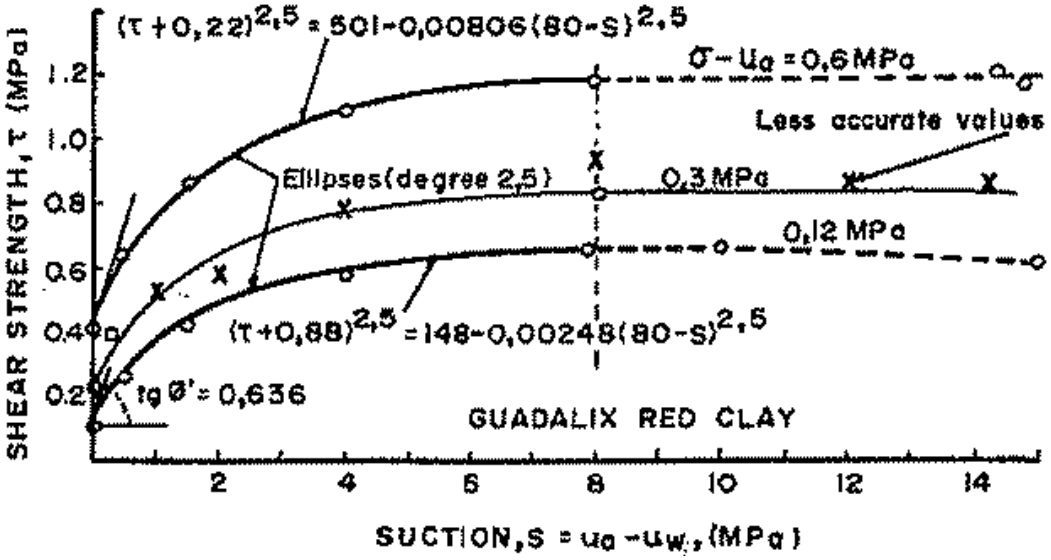

Fig. 2.9 Variation of shear strength with suction, for different values of vertical stress (direct shear tests) for Guadalix red clay (Escario and Juca 1989)

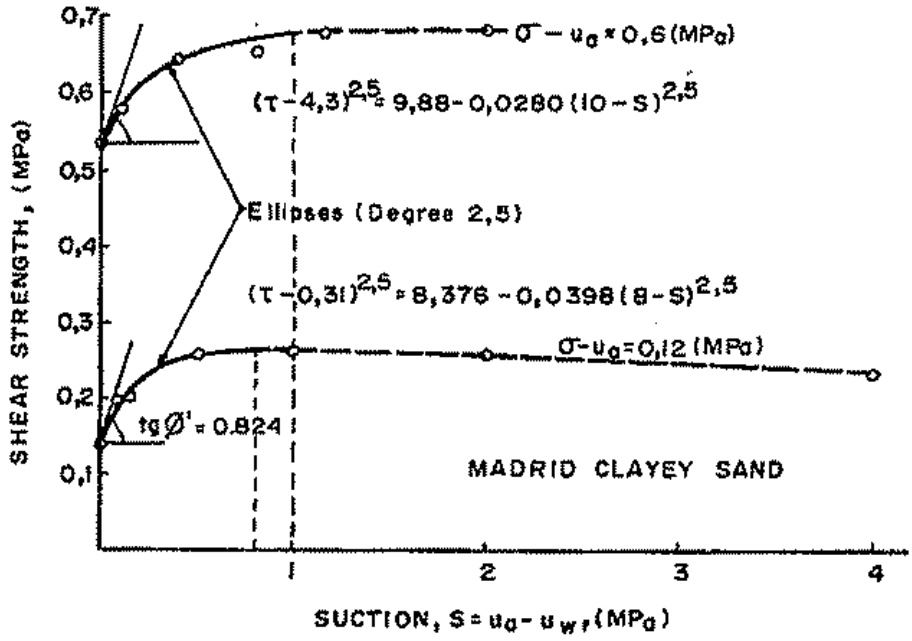

Fig. 2.10 Variation of shear strength with suction, for different values of vertical stress (direct shear tests) for Madrid clayey sand (Escario and Juca 1989)

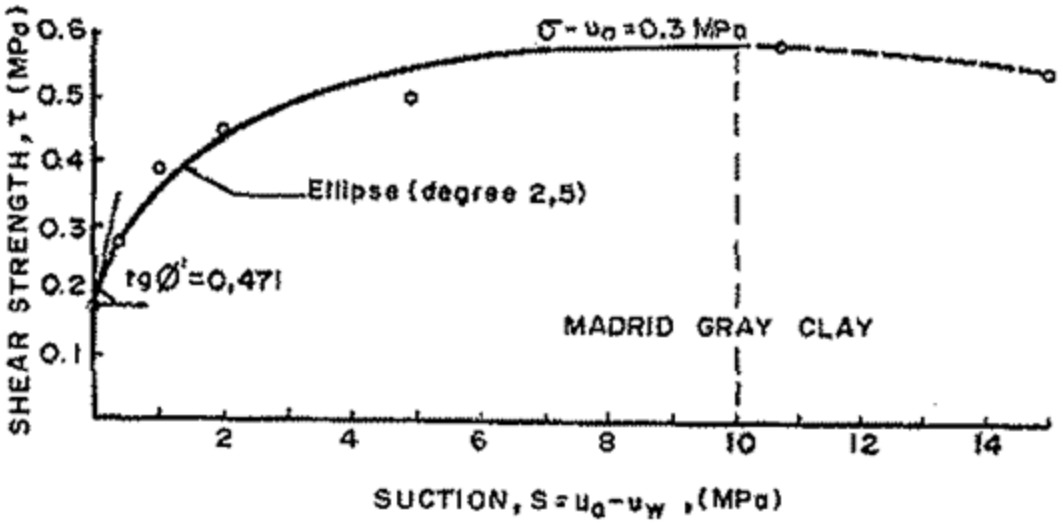

Fig. 2.11 Variation of shear strength with suction, for different values of vertical stress (direct shear tests) for Madrid gray clay (Escario and Juca 1989)

The plot for shear stress vs. vertical stress for Red clay and Madrid clayey sand is presented in figures 2.12 and 2.13.

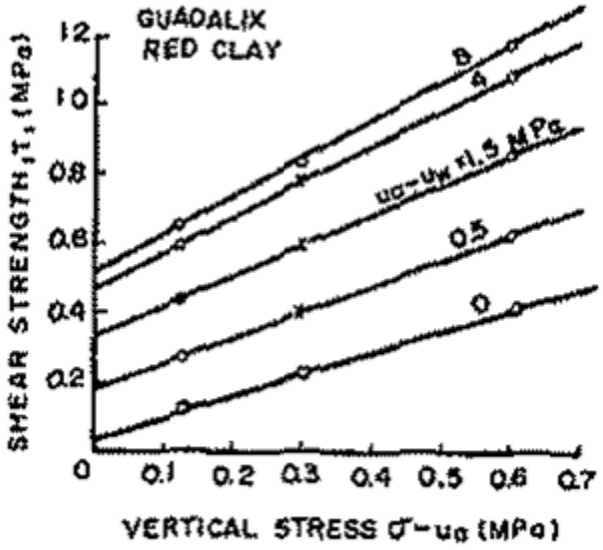

Fig. 2.12 Variation of shear strength with vertical stress, for different values of vertical stress (direct shear tests) for Guadalix red clay (Escario and Juca 1989)

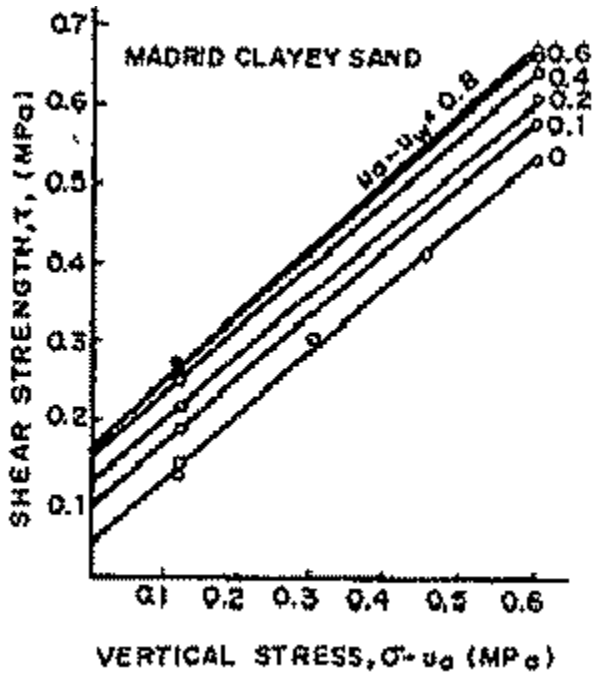

Fig. 2.13 Variation of shear strength with vertical stress, for different values of vertical stress (direct shear tests) for Madrid clayey sand (Escario and Juca 1989)

Using the data obtained from Escario and Juca (1989), Blight (1961) and Donald (1961), Likos and Lu (2004) developed the plot for χ vs. S_r which is presented in figure 2.14.

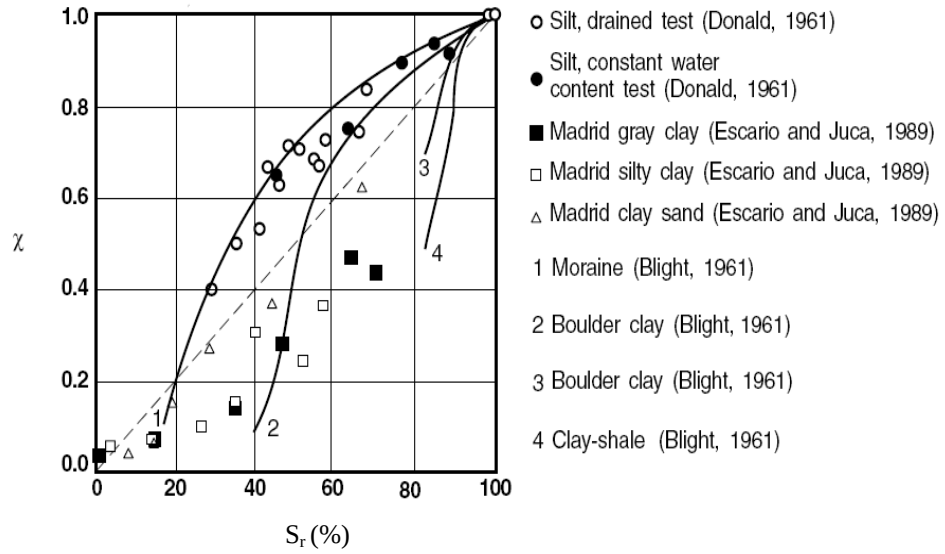

Fig. 2.14 Plot for χ vs. S_r (Likos and Lu 2004)

The analysis carried out by Öberg and Sällfors (1995) shall be discussed next. The theoretical and experimental results for cohesionless soil samples were studied in detail. A hypothesis was proposed in which it was reflected that χ parameter occupies only a fraction of pore area.

$$\chi = \frac{A_w}{A_{Tot}}$$

It was proposed that if u_a is equal to atmospheric pressure, the equation of shear strength equation for the unsaturated soil can be formulated as:

$$\tau = c' + \left(\sigma - \frac{A_w}{A_{Tot}} u_w \right) \tan \phi' \qquad (20)$$

An analysis was presented for ideal two and three dimensional soils and the plot for χ vs. S_r was studied as shown in figure 2.16. Sparks (1963) also obtained similar results figure 2.15.

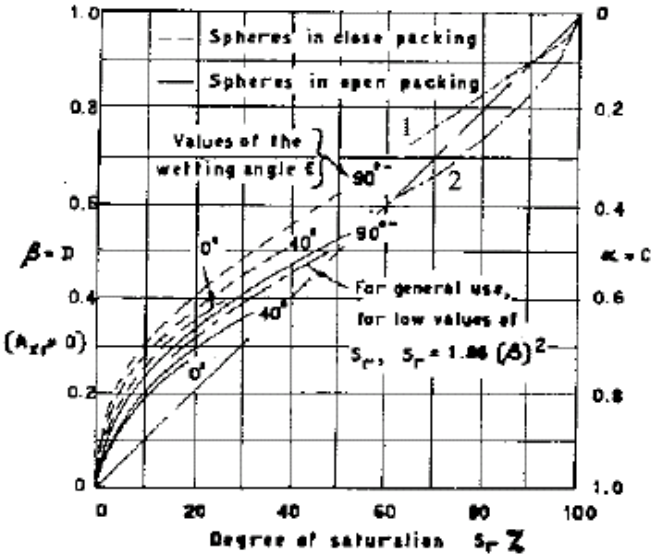

1. Theoretical, close packing, Öberg and Sällfors (1995)

2. Theoretical, open packing, Öberg and Sällfors (1995)

Fig. 2.15 Relationship between χ and S_r for idealized soils (Sparks 1963)

After studying the theoretical trend, the experimental results as obtained by Donald (1961) have been analyzed. And a similar trend was noted as can be seen in figure 2.16.

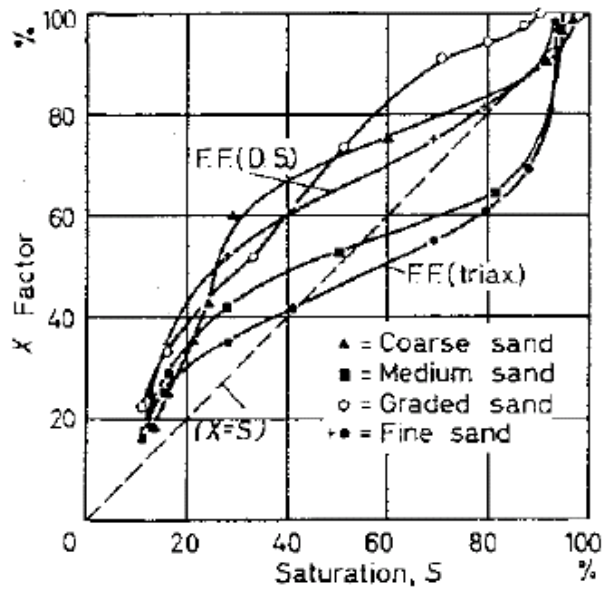

Fig. 2.16 Relationship between χ and S_r for sands (Donald 1960)

It was explained by the authors that the equation for shear strength could be written as:

$$\tau = c' + (\sigma - S_r * u_w) \tan \Phi' \quad (21)$$

Briaud et al. (2007) proposed the following:

$$\alpha = S_r$$

Thus, considering that is χ equal to S_r. It was noted that this equation was true for the cohesionless soils for a degree of saturation greater than 50%. They stated that the error on χ would be within 20% for most soils and the corresponding error in the shear strength would be smaller.

Öberg and Sällfors (1995) observed that the analysis for the fine grained soils was even more complex. The typical pore size distribution for the clayey material shows two characteristic pore sizes as seen in figure 2.17. The drainage of water from the pores is phenomenal. For example, for silty clay soil sample, water would drain from the larger pore spacing when desaturated. The tensile pore water pressure now acts on the large pores. The smaller size pores would remain unaffected at this stage. Higher suction values lead to the lower values of χ. Water is yet to be drained from the smaller pores. The water content and hence the degree of saturation remains high at this stage.

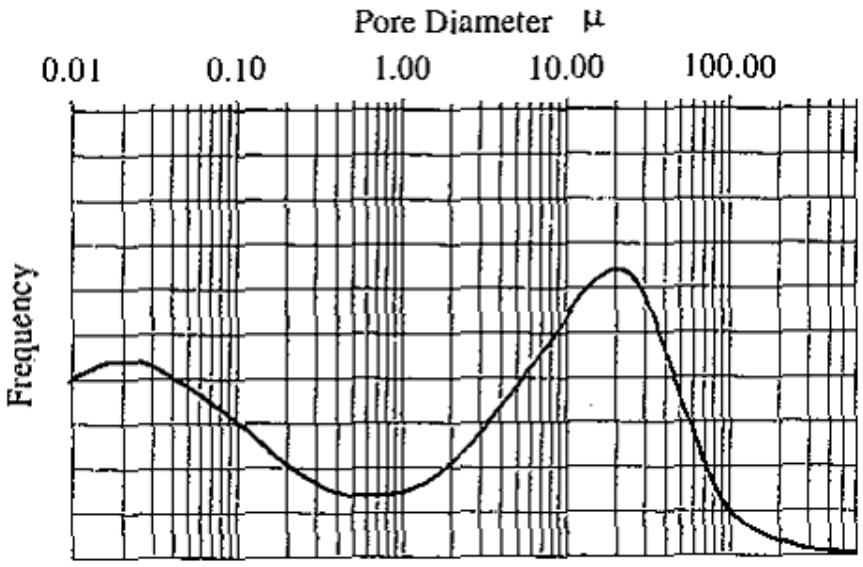

Fig. 2.17 Pore size distribution for a clay redrawn (Ahmed et al. 1974)

Thus, a need is felt to research on the situation for fine grained soils. A hypothesis is presented in the following section for understanding the complex nature for the fine grained sample and the unsaturated soil parameter is evaluated based on this equation. A detailed study is carried out on the fine grained clay sample and the results are presented which is in good agreement with the hypothesis.

2.6 Research hypothesis

The hypothesis for this research states that a unique relationship exists between the unsaturated shear strength parameter α and the degree of saturation for a specific soil specimen.

The hypothesis predicts the following equation to measure the shear strength of soil:

$$\tau = c' + (\sigma - f(S_r) * u_w) \tan \Phi' \qquad (22)$$

To achieve this objective, the shear strength of the unsaturated soil was determined using the conventional direct shear test apparatus. Shear stress was applied to the sample at a slow rate of strain horizontally such that the upper box moves relative to

the lower box at a controlled rate of strain. The shear stress response is monitored with the aid of force transducer. The vertical load is applied axially on the sample. The axial deflection is measured by a displacement transducer during the consolidation and shearing stage.

The direct shear apparatus was used to find the shear strength of the soil as its main advantage is that it is simple to use as compared to the triaxial test apparatus. Another advantage is that the sample size is smaller and it takes a shorter time to drain the sample.

The research so far has been conducted under controlled matric suction conditions. And this is done by modifying the apparatus. In this study, a simple and reliable technique was adopted where the sample was dried outside and the tensile stress was induced on the sample. The pore water pressure was estimated using the SWCC. The sample was consolidated for sufficiently long time in order to completely dissipate the excess pore water pressure by applying the normal stress slowly. The strain rate while shearing, was such that the drainage of the sample is controlled excess pore water pressure will not be generated. A detailed procedure is discussed in Chapter V.

CHAPTER III

MEASUREMENT OF ENGINEERING PROPERTIES OF THE SOIL UNDER THE STUDY

The complex nature of the clay has been studied and the physical and engineering properties of the soil are presented in this chapter. ASTM standard has been used to determine the properties under controlled laboratory conditions.

Fig. 3.1 Dark grey clay specimen

Elaborate tests were conducted on the specimen chosen for the study under controlled laboratory conditions. The dark grey clay specimen as seen in the figure 3.1 was used in this study. The engineering properties of the soil are discussed next.

3.1 Atterberg limits test

The Atterberg limits were determined in accordance with ASTM-D4318-00.

3.1.1 Liquid limit (LL) test on normally consolidated clay

The liquid limit of the specimen was determined using the Casagrande's apparatus. Table 3.1 gives the results obtained from the test. Figure 3.2 shows the plot between the water content vs. the number of blows used to obtain the liquid limit. The water content corresponding to 25 blows in the plot was measured as the liquid limit of the specimen.

Table 3.1 Determination of the water content of the sample corresponding to the number of blows

Number of blows	**Weight of wet soil + container (g)**	**Weight of container (g)**	**Weight of wet soil (g)**	**Weight of dry soil + container (g)**	**Weight of dry soil (g)**	**Weight of water (g)**	**Water content (%)**
14	28.92	15.1	13.82	25	9.9	3.92	39. 6
26	23.96	15.5	8.46	21.7	6.2	2.26	36.45
35	27.51	14.9	12.61	24.3	9.4	3.21	34.15

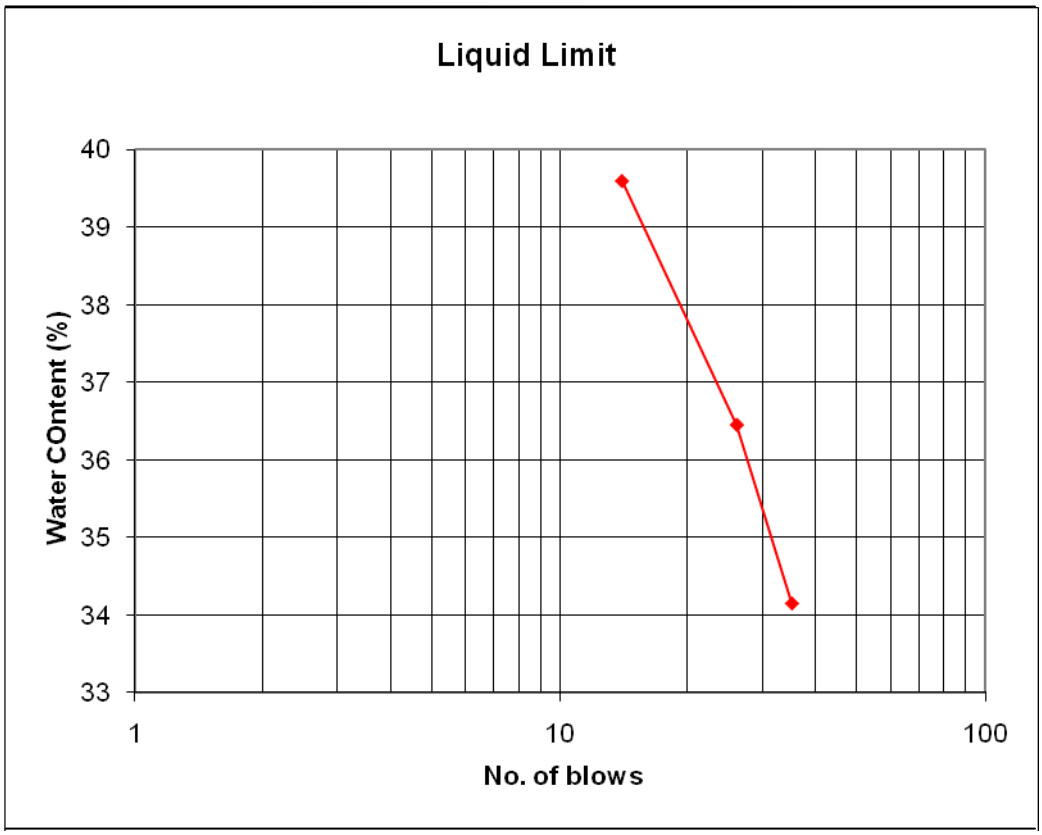

Fig. 3.2 Plot for liquid limit determination

The liquid limit for the soil sample was determined as 36.81%.

3.1.2 Plastic limit (PL) test on normally consolidated clay

Table 3.2 gives the experimental results to obtain the plastic limit of the sample.

Table 3.2 Determination of plastic limit

Weight of wet soil + container (g)	Weight of container (g)	Weight of wet soil (g)	Weight of dry soil + container (g)	Weight of dry soil (g)	Weight of water (g)	Water content (%)
21.62	15.25	6.37	20.6	5.35	1.02	19.07
24.35	15.33	9.02	22.9	7.57	1.45	19.15

The plastic limit of the soil sample was determined as 19.1%.

Plasticity Index (PI) = LL – PL = 36.81% - 19.1% = 17.71%

3.2 Specific gravity

The specific gravity of the solid particles (G_s) is defined as the ratio of mass of a given volume of solids to the mass of an equal volume of water at 4^0C.

$$G_s = \frac{\rho_s}{\rho_w}$$

where,

ρ_s – mass density of soil solids

ρ_w – mass density of water

The test is performed in accordance with ASTM-D854-00. The pycnometer is used for this purpose. The specific gravity was found to be 2.65.

3.3 Soil classification

Based on Unified Soil Classification System (USCS), the soil is classified as CL (low plasticity clay). Thus, this clay shows a very small potential to swell (PI<75%).

3.4 Particle size analysis

The particle size analysis is carried out using hydrometer since the size of the fine-grained soil was less than 75µ. The plot for percentage finer vs. diameter of the particles is shown in figure 3.3. The diameter of the particle was determined as 0.089 mm from the hydrometer test by taking its weighted average. Table 3.3 gives the test results for the hydrometer test.

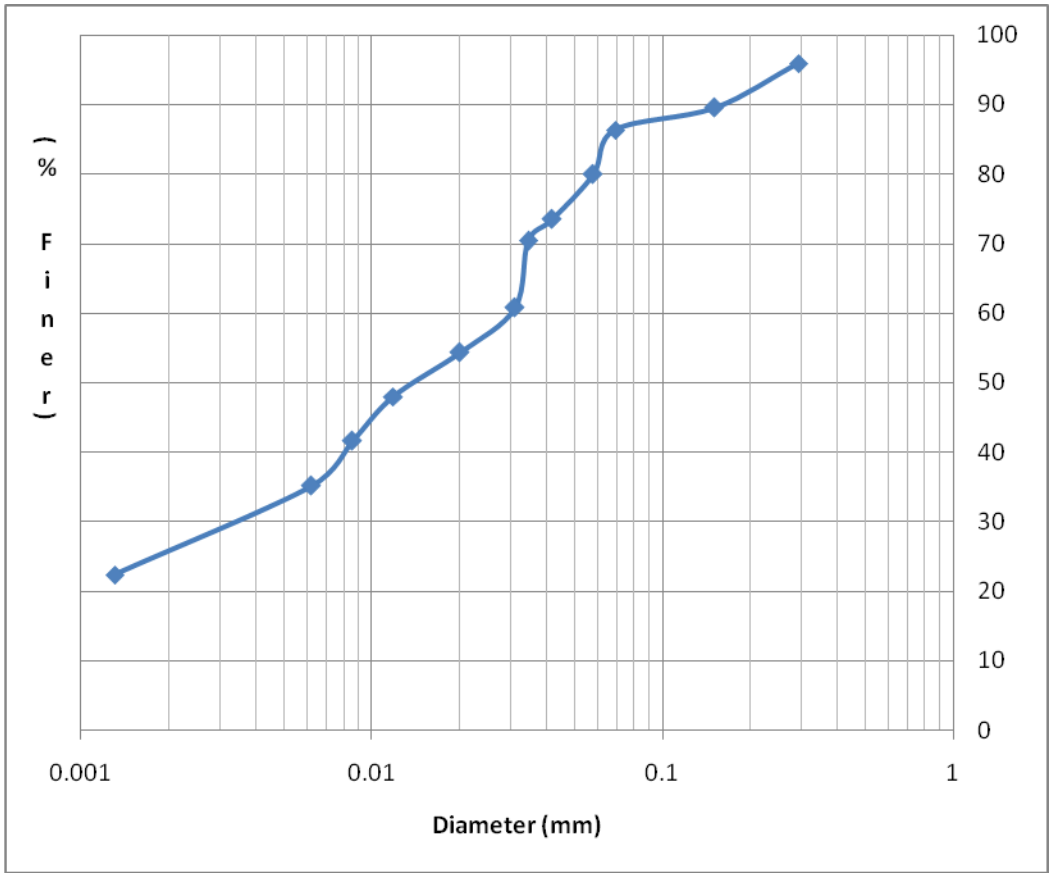

Fig. 3.3 Hydrometer analysis

Table 3.3 Particle size analysis using hydrometer

Time (seconds)	Time (minutes)	Actual hydrometer reading	Composite correction	Hydrometer reading – correction	Temperature (^{0}C)	Effective hydrometer Depth	K from table	Diameter of the particle (mm)	% Finer in suspension
1	0.017	1.033	0.003	1.03	23	8.4	0.01309	0.3	96.287
4	0.067	1.031	0.003	1.028	23	8.9	0.01309	0.15	89.87
20	0.33	1.03	0.003	1.027	23	9.2	0.01309	0.069	86.66
30	0.5	1.028	0.003	1.025	23	9.7	0.01309	0.058	80.24
60	1	1.026	0.003	1.023	23	10.2	0.01309	0.042	73.82
90	1.5	1.025	0.003	1.022	23	10.5	0.01309	0.035	70.61
120	2	1.022	0.003	1.019	23	11.3	0.01309	0.032	60.98
300	5	1.02	0.003	1.017	23	11.8	0.01309	0.0201	54.56
900	15	1.018	0.003	1.015	23	12.3	0.01309	0.0119	48.144
1800	30	1.016	0.003	1.013	23	12.9	0.01309	0.0086	41.72
3600	60	1.014	0.003	1.011	23	13.4	0.01309	0.0062	35.30
86400	1440	1.01	0.003	1.007	23	14.4	0.01309	0.00131	22.47

Table 3.4 Summary of test results

Test	**Result**
Liquid limit	36.81%
Plastic limit	19.1%
Plasticity index	17.71%
Color	Dark grey
Specific gravity	2.65
Soil classification	CL

Table 3.4 gives the summary of the test results to obtain the engineering property of the specimen chosen for the study.

CHAPTER IV

DETERMINATION OF SOIL WATER CHARACTERISTIC CURVE

Significant research has been carried out to understand and measure the tensile pore water pressure. Various methods have been developed to measure the tensile pore water pressure of the soil. Some of the widely used methods include filter paper, psychrometers, tensiometers, pressure-plate apparatus, chilled mirror dew point, Decagon WP4 Dew point potentiometer and salt solution equilibrium test. But some of them have shortcomings as regards the reliability, economy and range of applications. The salt equilibrium method was used to measure the soil suction which is one of the most reliable and simple technique. The salt solution method also has the added advantage of being useful in determining the suction stress over the entire range of suction values.

Likos and Lu (2002) have stated that the positive pore water pressure is responsible for pushing the soil grains away from each other, whereas the negative pore water pressure pulls the soil particles close to each other. Thus, soil suction can be described as the measure of the ability of a soil to hold and attract water.

Fredlund and Rahardjo (1993) define soil suction as the free energy state of soil water and that it can be measured in terms of the partial vapor pressure of the soil water. In geotechnical engineering, the total suction comprises of two suction components, matric suction and osmotic suction. The total suction is defined as:

$$\psi = (u_a - u_w) + \Pi \qquad (22)$$

where,

ψ = total suction

$u_a - u_w$ = matric suction

Π = osmotic suction

u_a = tensile pore air pressure

u_w = tensile pore water pressure

Bulut and Wray (2005) state that the matric suction values depend on capillarity, texture and surface adsorption forces of the soil and osmotic suction depends on

dissolved salts concentration contained in the soil water. The capillary rise due to matric suction is explained using figure 4.1.

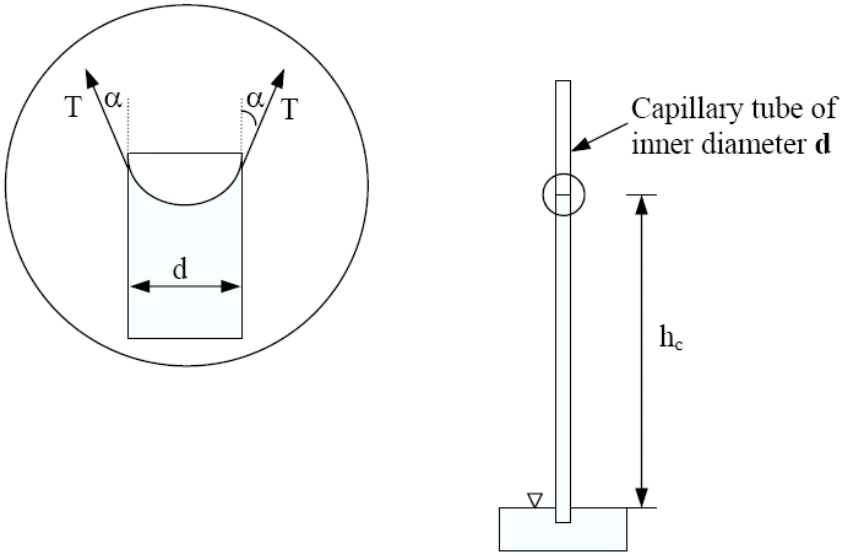

Fig. 4.1 The capillary rise due to matric suction (Sivakugan 2004)

And the maximum height of water in capillary tube is given as:

$$h_c = \frac{2T}{\rho_w g R_s} \qquad (23)$$

where,

R_s = Radius of curvature of the meniscus (i.e. d/2 cos α)

4.1 Soil water characteristic curve

Likos and Lu (2004) describe the soil water characteristic curve (SWCC) as the thermodynamic potential of the soil pore water with respect to the free water as a function of the amount of water adsorbed by the soil system.

A typical unimodal SWCC, as shown in figure 4.2 is the plot between gravimetric water content and the soil suction. Three zones can be identified from the SWCC that are explained below:

1. *Capillary saturation zone*

   The soil is saturated in this zone due to capillary action. But, tensile pore water pressure is exerted in the soil in this zone.

2. *Desaturation or funicular zone*

   In the desaturation zone, air increasingly displaces liquid water within the pores.

3. *Zone of residual saturation*

   In this zone, the liquid water is tightly held to the soil and the moisture movement in the soil is observed in the form of vapor flow. Some water movement in the form of film flow may be observed in this zone; also little hydraulic flow of water may occur through the pores.

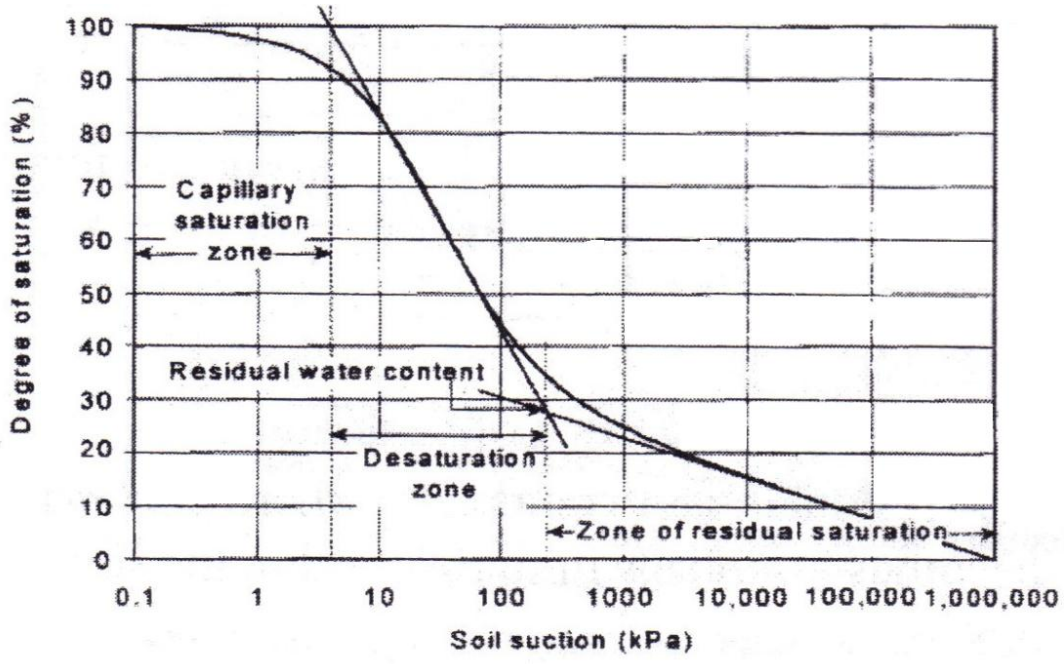

Fig. 4.2 Soil water characteristic curve illustrating the region of saturation (Briaud et al. 2007)

4.2 Salt equilibrium test

The salt equilibrium test was used to determine the SWCC for the soil sample. The working principle, the procedure, the necessary precautions taken during the test shall be discussed next.

4.2.1 Principle of the test

The salt equilibrium test is based on the thermodynamic relation between the osmotic suction and relative humidity of water. The tensile stress is induced in the sample in a controlled manner. This is done by using a predetermined salt concentration and allowing the sample to reach equilibrium in a sealed glass jar in an environment with minimum temperature fluctuations.

4.2.2 Precautions

The tensile pore water pressure was noted to be the most sensitive parameter in the effective stress equation of unsaturated soils and hence precautions were taken while measuring it. The picture detailing the equilibrium jar is seen in figure 4.3.

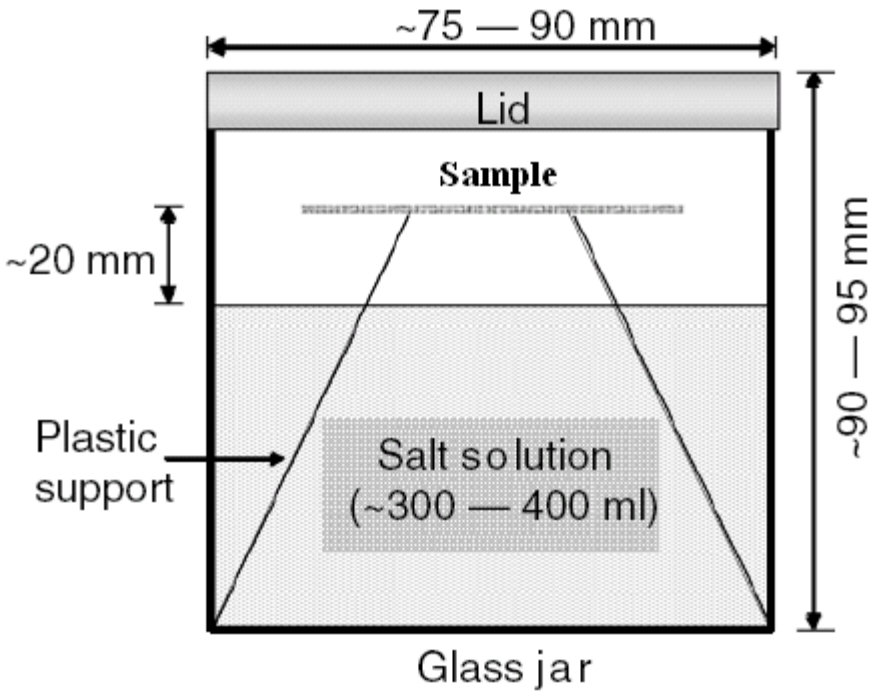

Fig. 4.3 Salt equilibrium jar redrawn (Bulut and Wray 2005)

1. The hysteresis effect exists in the SWCC. Hence, to maintain the curve in the drying state, the sample was inundated for a period of 24 hours.
2. During the equilibrium period, no change in the salt solution concentration was allowed. This was done by taking a large amount of solution in each jar. Thus any transfer of water into the sample or into the volume of air as water vapor was taken care of.
3. The distance between the sample and the surface of the solution was about 20mm as seen in the figure 4.3.
4. The empty air volume in each glass jar was kept minimal.
5. Sufficient time was allowed for the sample to reach equilibrium and the lid of the glass jar was tightly sealed.
6. The dimension of the glass jar was chosen to be small enough in order to ensure same water pressure and hence relative humidity at all heights.
7. The experiment was carried out in an environment subject to minimum temperature fluctuations.

8. The water content of the sample was measured as quickly and as accurately as possible at the end of the salt solution test.
9. Distilled water was used as a solvent in the test.
10. The size of the sample was small enough in order to let the sample reach equilibrium.

4.2.3 Test procedure

The test was performed in accordance with the calibration technique for filter paper using the salt equilibrium procedure as described by Bulut and Wray (2005). Magnesium chloride, 6-Hydrate, crystal ($MgCl_2.6H_20$) was used as the solute and distilled water was used as the solvent to prepare the salt solution. Bulut et al. (2001) studied that a smaller quantity of $MgCl_2.6H_20$ is efficient to induce higher suction values. The samples were kept in the aluminum cups inside the jar. Five such cups were kept in each jar. This was done in order to obtain the average water content for each jar corresponding to a specific suction value. The SWCC was then obtained as a plot between the average gravimetric water content and the suction stress induced due to the salt concentration. The typical salt equilibrium jars are shown in figure 4.4.

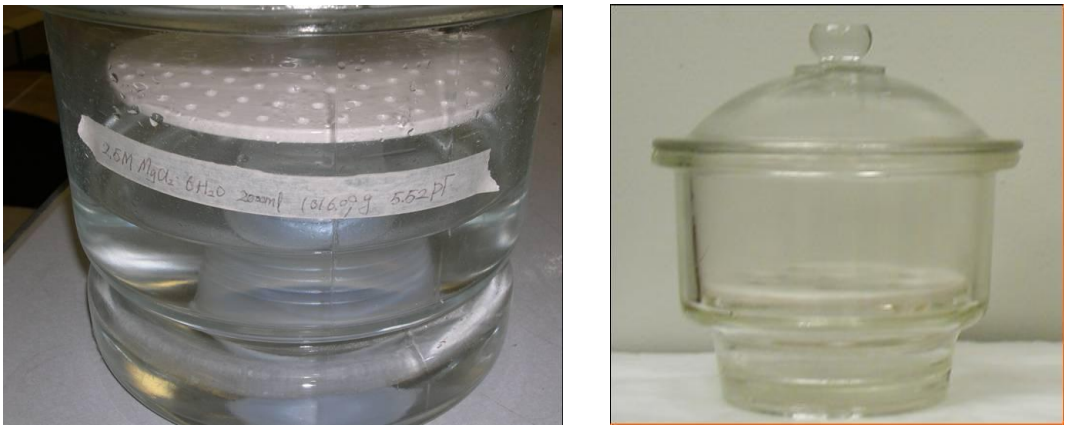

Fig. 4.4 Salt equilibrium jar (Briaud et al. 2007)

Steps in the procedure are as follows:

1. According to the table 4.1, the soil suction values were chosen and the mass of solute was calculated.
2. 2000 ml of distilled water was used as the solvent to prepare the salt solution by mixing the salt with the stirrer. It was ensured that the salt concentration is maintained uniform.
3. The soil samples were inundated for a period of 24 hours.
4. These soil samples were kept in the aluminum cups. 4 cups were placed on the perforated ceramic plate in each jar to obtain the average water content of the soil samples after equilibrium.
5. A period of 14 days was allowed for the samples to reach equilibrium.
6. The water content of the samples was determined immediately after the test.

The suction potentials were chosen based on the requirements of the test. The following table indicates the suction generated from the test by selecting a corresponding molality. Table 4.1 summarizes the determination of mass of salt corresponding to the suction value.

Table 4.1 Determination of mass of salt for the required suction values.

Molality (moles/kg)	**Moles of solute $MgCl_2.6H_2O$ for 2000 gm of solvent (Molality * Weight of solvent)**	**Molecular mass of $MgCl_2.6H_2O$**	**Mass of $MgCl_2.6H_2O$ required (Moles of solute * Molecular mass of $MgCl_2.6H_2O$)**	**Suction potential generated (kPa)**
0.001	0.002	203.31	0.407	7
0.002	.004	203.31	0.8132	14
0.02	0.04	203.31	8.132	133
0.2	0.4	203.31	81.32	1303
1.5	3.0	203.31	609.9	14554
2.5	5.0	203.31	1016.56	32776

4.2.4 Test measurement

The main measurement of this test was to measure the water content of the soil sample for each jar and take its average. The best curve fit was then obtained to indicate the relation between the water content and the soil suction. Table 4.2 represents the water content the soil sample was left with after it reached equilibrium.

$$W\ (\%) = \frac{W_w}{W_s} * 100 \qquad (24)$$

where,

W = Water content of the sample (%)

W_w = Weight of water (g)

W_s = Weight of solids (g)

Table 4.2 Determination of average water content values from the salt test

Suction (pF)	Average water content (%)
0	24.91
2.14	21.53
4.115	18.77
5.163	8.31
5.515	4.92

The soil water characteristic curve for the dark grey clay specimen is obtained. The plot is analyzed in Chapter VII.

4.2.5 Test interpretation

The lower the water content, lower is the pore water potential compared to the free water and the soil suction is high. And at higher water content, the difference between the pore water potential and the potential of free water decreases and the suction value is low. The soil suction corresponds to zero when the potential of the pore water is equal to the potential of free water.

CHAPTER V

DETERMINATION OF UNSATURATED SHEAR STRENGTH OF CLAY

One of the major goals in this study is the shear strength determination of the normally consolidated dark grey clay specimen. The shear strength is determined using the direct shear apparatus. The shear strength parameters c' and Φ' are determined for full saturation and are assumed to be independent of degree of saturation. The test was performed in consolidated drained manner. The rate of strain was determined such that the excess pore water pressure is not generated during shear. The principle of direct shear test, rate of strain determination and test procedure are discussed in this chapter.

5.1 Principle of the test

The apparatus consists of a box split in two halves. The lower box moves relative to the upper box at a pre-determined rate of strain. The figure 5.1 shows the working principle of direct shear experiment. The normal load (P_z) is applied to the specimen through the rigid loading cap. Direct shear force (P_x) is applied to the sample and the failure is observed on the horizontal plane (AB). The shear force, normal displacement and horizontal displacement are measured during the test. The shear stress (τ) and normal stress (σ_n) are obtained by dividing the shear force and normal force by the cross-sectional area of the cylindrical specimen.

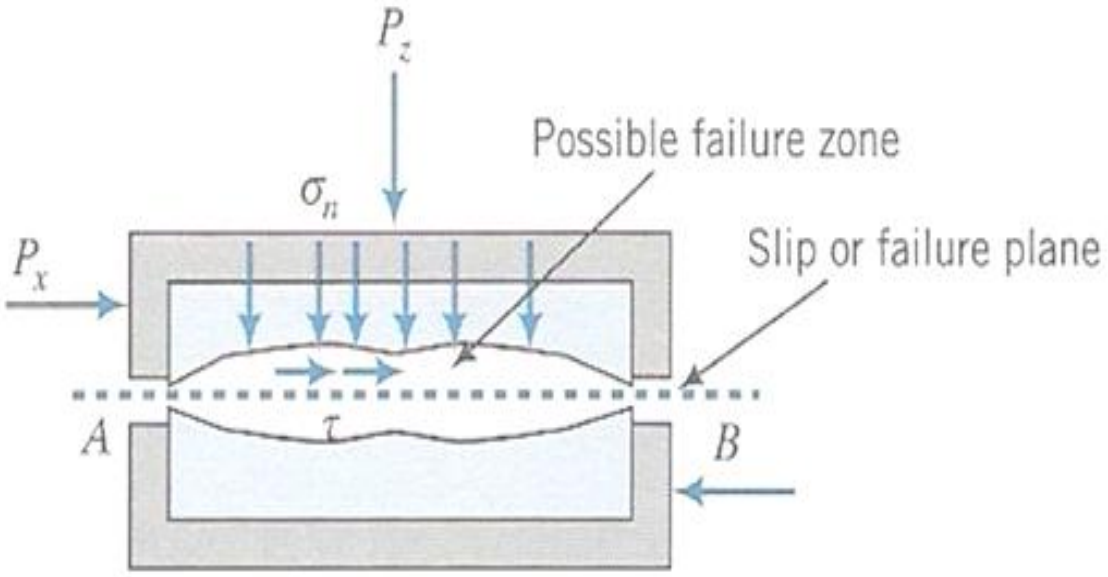

Fig. 5.1 Shear box (Budhu 2000)

5.2 Assumptions

1. The shear strength parameters c' and Φ' for the dark grey clay specimen are independent of degree of saturation and their values are determined at full saturation.
2. The failure occurs on the horizontal plane formed at the intersection of the upper and lower box.

5.3 Advantages of DST

The direct shear test has the following advantages over the triaxial test:

1. It is a very simple test.
2. The drainage length is small.
3. The soil type selected for the study being fine grained, leads to greater time to failure in case of triaxial tests.
4. The cavitations problems are not seen while saturating the sample.

5.4 Selection of the strain rate

The literature survey for the shear strength determination on saturated clay specimens was conducted. The strain rate adopted for the study was 0.0005 mm/min. The time to failure for the sample was observed at the end of three days.

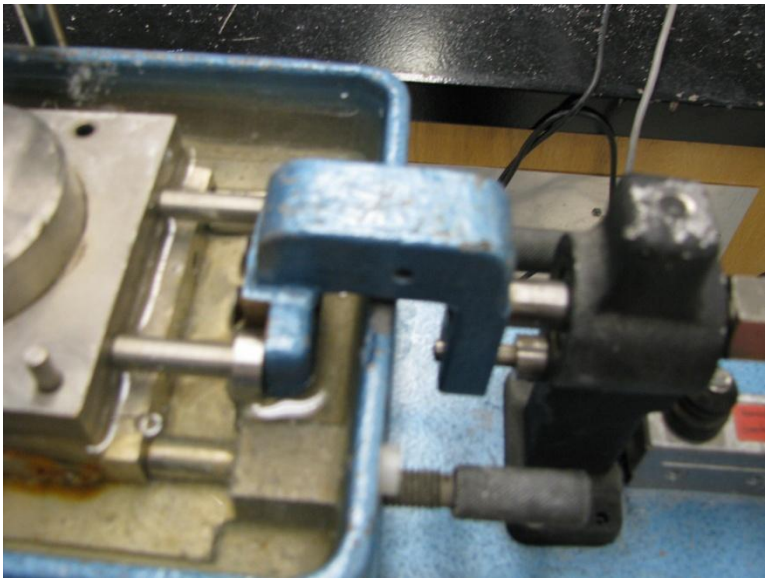

Fig. 5.2 Shearing of the saturated sample

The following table by Fredlund and Rahardjo (1993) was studied and a conservative rate of strain was adopted for the study based on the time to failure of the sample.

Table 5.1 Review on strain rate adoption (Fredlund and Rahardjo 1993)

	Direct shear test	Displacement rate d_h	Displacement at failure, d_h†	References
		mm s^{-1}	mm	
Madrid gray clay	CD	1.4×10^{-4}	3.5–5	Escario (1980)
Madrid gray clay	CD	2.8×10^{-5}	6.0–7.2	Escario & Sáez (1986)
Red clay of Guadalix de la Sierra	CD	2.8×10^{-5}	4.8–7.2	Escario & Sáez (1986)
Madrid clayey sand	CD	2.8×10^{-5}	2.4–4.8	Escario & Sáez (1986)
Glacial till	CD (multistage)	1.7×10^{-5}	1.2	Gan (1986)

† Square specimen of 50 by 50 mm.

5.5 Sample preparation

The cylindrical sample was trimmed using the wire saw. Care was taken to not to disturb the clay sample. The size of the sample on average was 62 mm in diameter and 26 mm in height. The trimmed sample is shown in figure 5.3.

Fig. 5.3 Soil sample for DST

5.6 Test procedure

The test was performed in accordance with ASTM D 3080-04, standard procedure. A typical direct shear box assembly is shown in figure 5.4. The samples were stored in the controlled laboratory conditions with the humidity approximately equal to 98%. The samples were saturated in the water bath. The normal load was applied to the specimen for a period of 24 hours. The axial displacement was monitored. The sample was then sheared. The shear force and axial displacement were measured and suitable plots were obtained for analysis. Steps in test procedure are discussed next.

Fig. 5.4. Direct shear box assembly (Biscontin 2006)

5.6.1 Saturated soil samples

1. The shear box was assembled. The box arrangement was such that it prevented torque from being applied to the sample. Damp porous stones were used at the top and bottom of the sample to allow two-way drainage of the sample. The diameter of the porous stone was 60 mm. The permeability of the porous stone was greater than that of the specimen being tested. Also, the texture was fine enough to prevent excessive intrusion in the soil sample. The porous stone was also used to transfer the horizontal stress to the sample and hence it was chosen to be coarse

enough to provide an interlock with the sample without allowing any stress concentrations. The loading cap was placed on top of the porous stone. The box is adjusted such that it just touches the shear force loading system. No load was allowed to be imposed on the load measuring system.

2. The cylindrical sample was placed inside the box between the two porous stones. The diameter of the box was 62 mm. The screws were given $1/4^{th}$ rotation to reduce the friction between the two boxes. The non-corrosive shear box was placed inside the water bath. The sample was kept saturated till the end of the test by adding water in the water bath. The wet sample used to determine the shear strength coefficients is shown in figure 5.5.

Fig. 5.5 The dark grey wet clay sample

3. The loading yoke was placed on the sample and was adjusted horizontal. A small normal load was applied to the specimen. It was verified that all components of the loading system are seated and aligned so that movement of the load transfer plate into the shear box is not inhibited. A normal load of 6.5 kg was applied on the specimen through the loading yoke by activating masses on it. The load was

applied till the vertical displacement leveled off thus ensuring complete dissipated of excess pore water pressure.

4. The data acquisition system was accomplished by using linear strain conversion transducer (LSCT) and force transducer. The LSCT first converts the displacement into electric voltage output. Similarly, the force is converted into electric voltage output. The data is recorded using Notepad at regular intervals by making use of a Labview program, GGeotech written by Dr. Giovanna Biscontin. The vertical displacement was monitored using LSCT and the shear force was monitored using force transducer. The axial displacement was monitored immediately after the loading was applied to the sample.

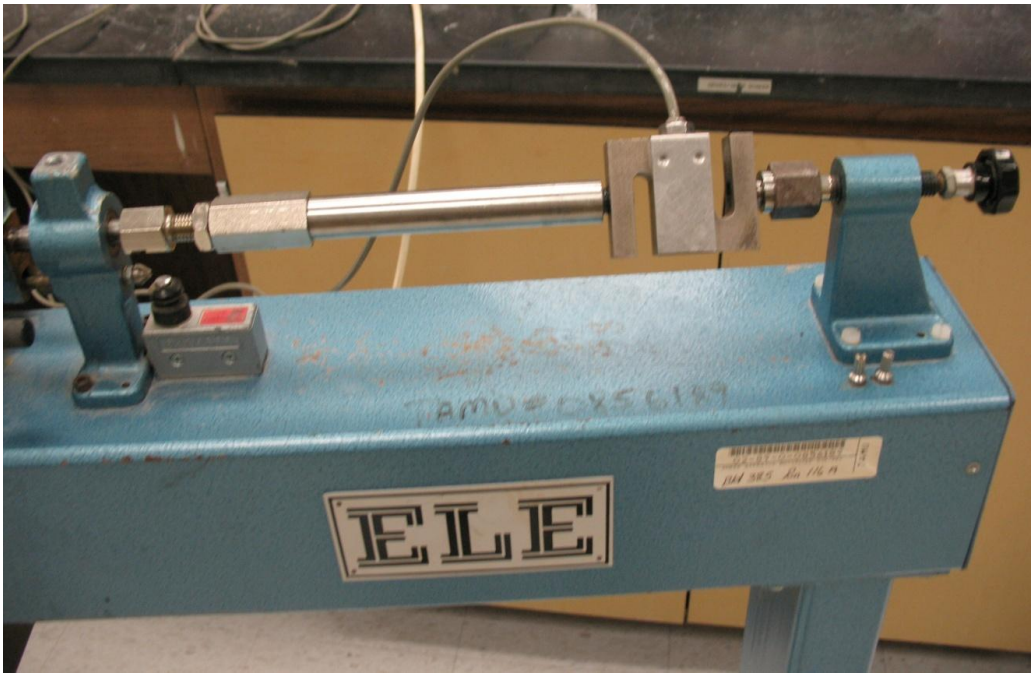

Fig. 5.6 Force transducer to monitor the response of applied shear force

5. The uniform rate of strain was applied by using the gear box arrangement. The rate of strain of 0.0005 mm/min. was used to the specimen by setting the third gear.

6. The shearing was continued till the shear resistance measured by the sample leveled off.
7. The test was then repeated for 52.15 kPa and 90.08 kPa normal stresses.

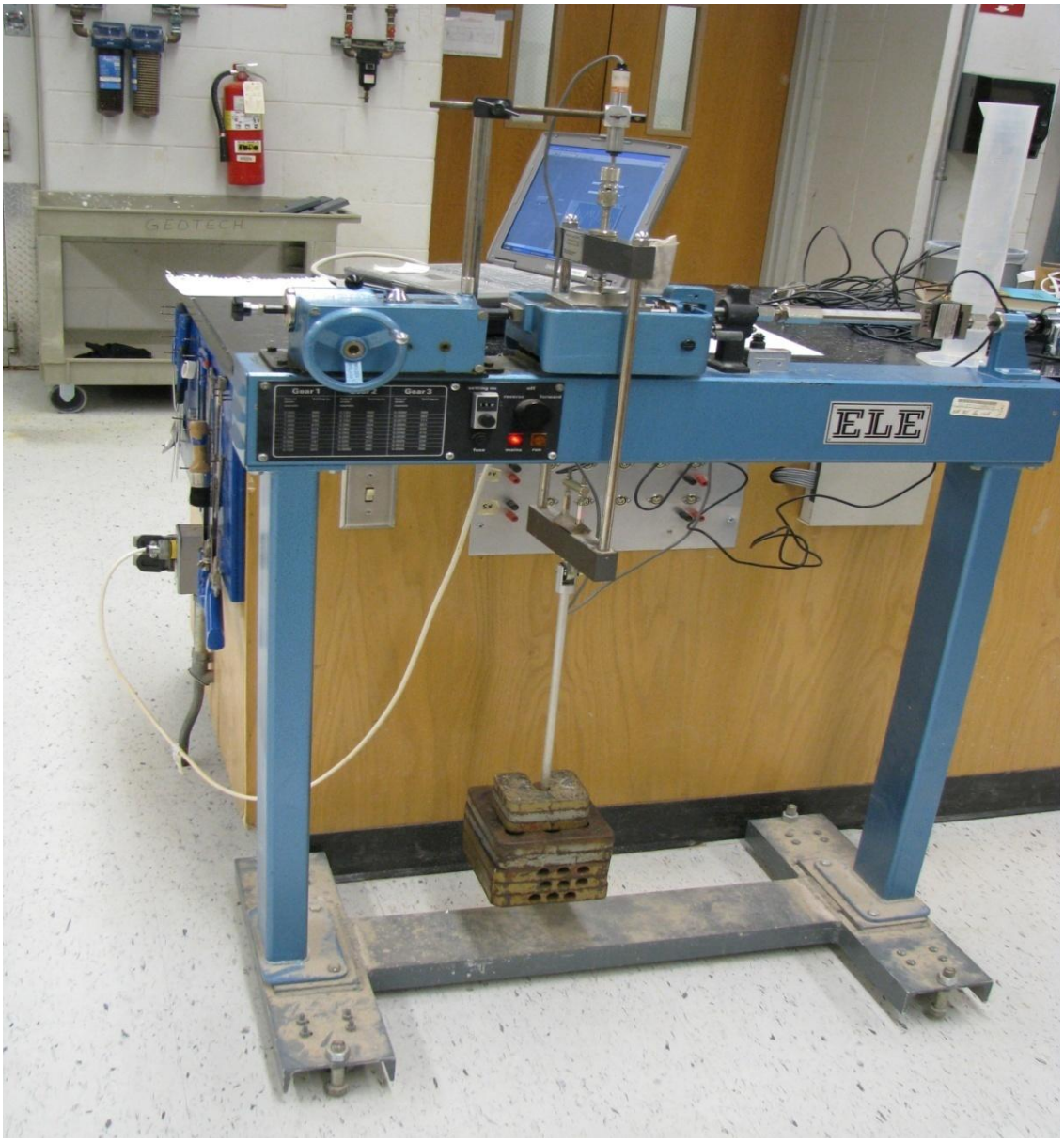

Fig. 5.7 The direct shear test setup

5.6.2 Unsaturated soil samples

The procedure for unsaturated was the same as saturated with one difference that the sample was allowed to dry and thus suction was induced on these samples. The dried sample can be seen in figure 5.8. The samples were dried outside for different pre-determined hours and then placed inside the shear box. The normal load of 6.5 kg was applied to all the samples till the displacement leveled off. The sample was sheared at rate of strain of 0.00365 mm/min.

After the sample had failed, the sample was cut along the failure plane and a portion of the sample was taken from the failure plane for the water content determination. While running the test, it was ensured that the sample did not lose moisture content after it was placed in the box. This was done by keeping damp cloth on the box throughout the experiment.

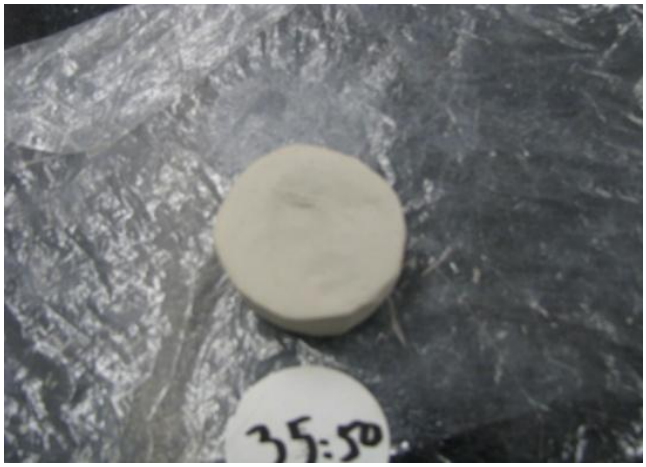

Fig. 5.8 The light grey color drier clay sample which was dried for 35 hours 50 minutes

The analysis of the data collected is presented in Chapter VII.

CHAPTER VI

RESEARCH METHODOLOGY

6.1 Introduction

Attempts have been made by various research workers to study the complex nature of fine-grained soil especially to determine the unsaturated soil shear strength and establish a realistic equation for shear strength in terms of unsaturated shear strength parameter. Such unique relationships help in arriving at the actual shear strength of soil mass at various saturation levels without physically performing the tests on the samples. In the present study, the relationship between the parameter α and S_r for the selected clay sample is formulated.

The shear strength for fine grained clay sample could be determined:

1. as per the equation advocated by Briaud et al. (2007)
2. using the tensile pore water pressure determined by SWCC and
3. adopting the relation between the α and S_r

The research methodology adopted for this purpose will be discussed in this chapter.

6.2 Methodology

The direct shear test was conducted on the saturated normally consolidated clay sample. The shear strength parameters c' and Φ' were obtained from this test. The test was carried out in controlled laboratory conditions in a consolidated drained manner. To determine the unsaturated shear strength of the sample, it was dried outside the box for a predetermined number of hours.

When the sample was cut after drying, it was observed that the sample was drier on the outer side and was wet inside. Hence, the pore water pressure for the sample was defined by taking water content of the specimen on its failure plane.

The direct shear test was then carried out on the dried sample. The sample was subjected to horizontal shearing and the response was monitored using the force transducer. The plot for shear stress vs. the horizontal displacement was then obtained using MATLAB.

The test was performed in an environment where the temperature fluctuation was less than 1^0 C. The soil sample was kept in the box in such a way as to avoid any torque being applied, during shearing. For the drained condition, the shear strength of the fully saturated soil is given as:

$$s = \sigma' \tan \Phi'$$

$$c' = 0$$

Thus, the shear strength parameter, Φ' was determined from this test. For the unsaturated soils, the effective stress equation advocated by Briaud et al. (2007) is:

$$\sigma = \sigma' + \alpha * u_w + \beta * u_a$$

The test was carried out at atmospheric pressure and thus u_a was equal to zero.

$$\sigma' = \frac{s}{\tan \Phi'}$$

The water content was obtained by taking a small portion of the sample from the failure plane. The tensile pore water pressure corresponding to this water content was obtained from the SWCC. The summary for the research methodology is indicated in the form of flowcharts and is presented next.

6.3 Summary using flowcharts

Flowchart 1: DST on saturated clay

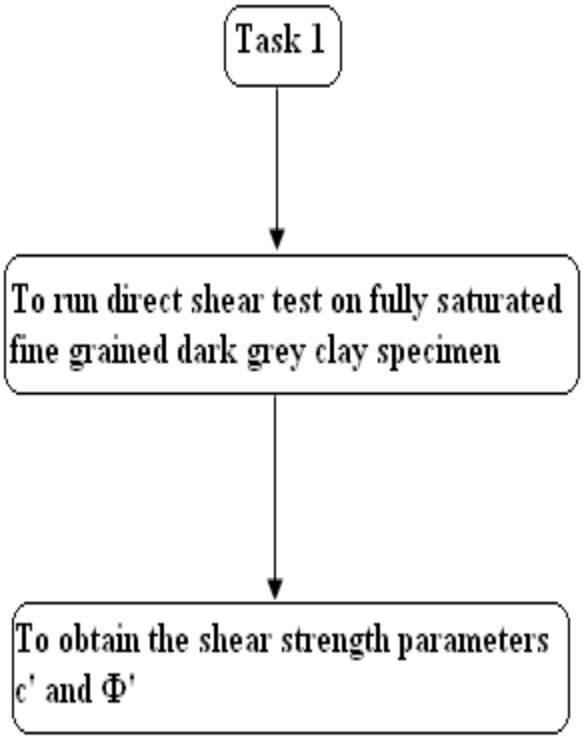

Flowchart 2: Determination of SWCC

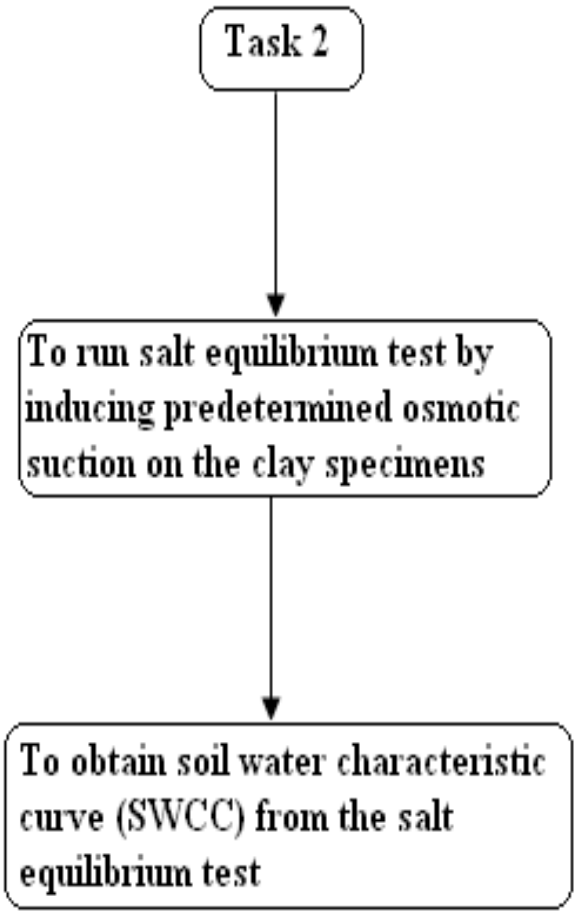

Flowchart 3: Determination of unsaturated shear strength parameter α for the clay specimen under study

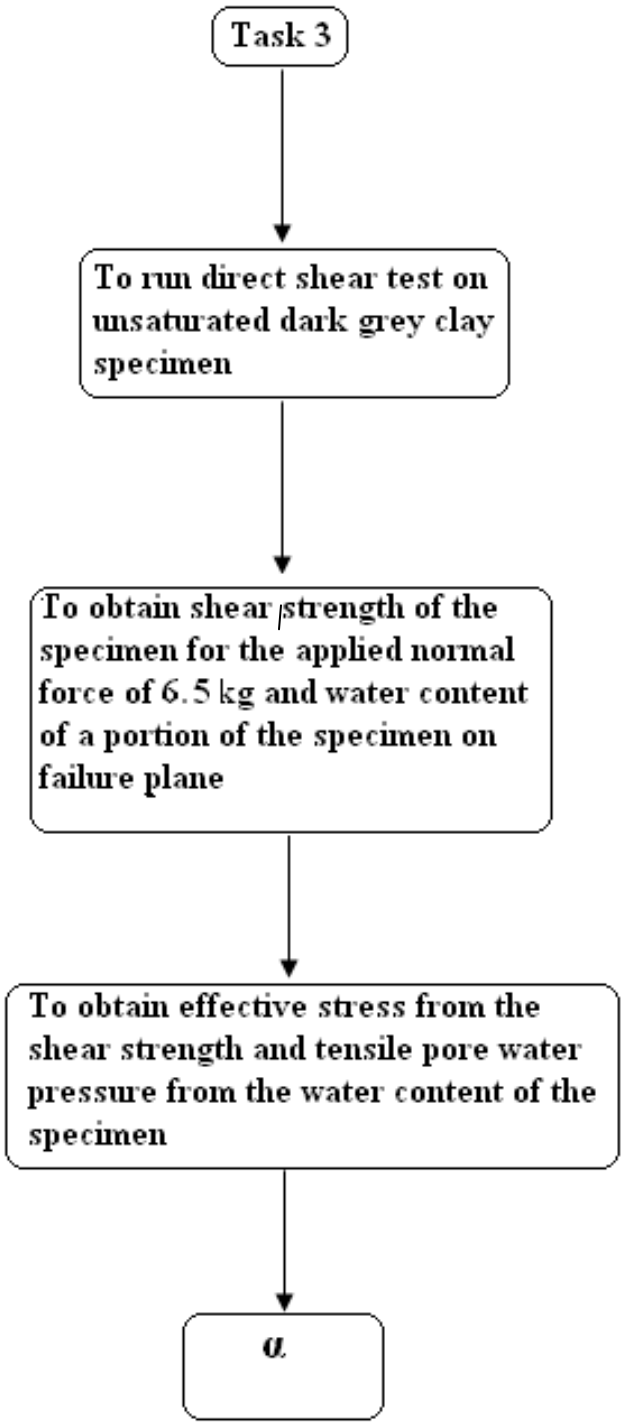

Flowchart 4: Determination of degree of saturation

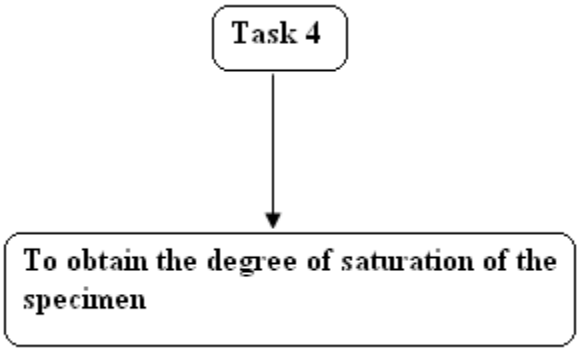

Flowchart 5: Determination of shear strength equation for unsaturated clay specimen

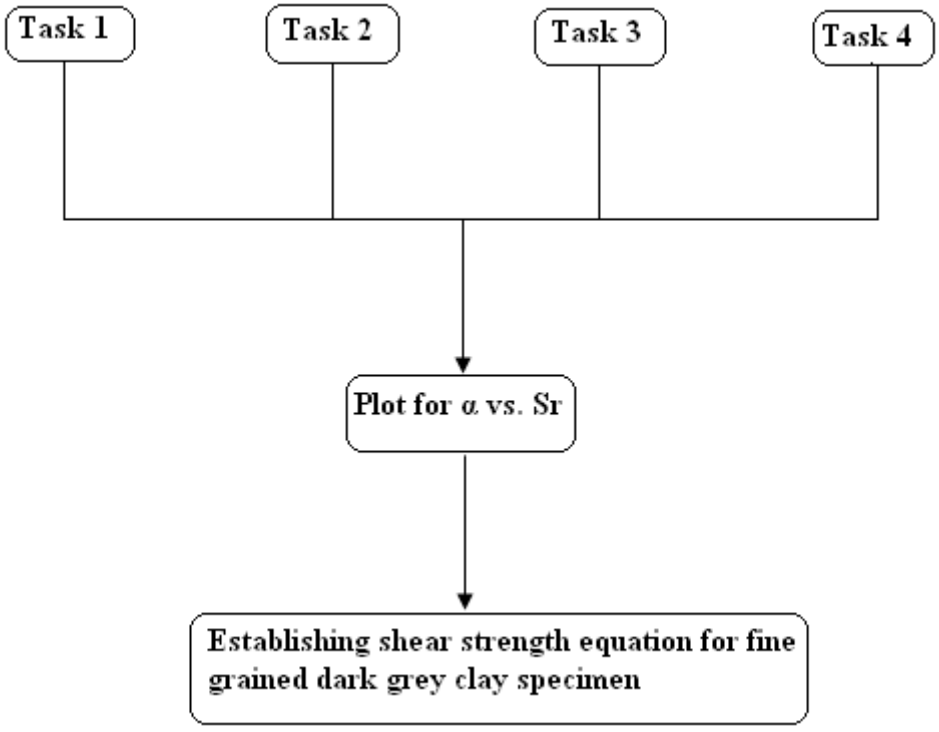

CHAPTER VII

PRESENTATION AND ANALYSIS OF STUDIES

The main objective of the investigation was to study the change shear strength and other characteristics at various states of drying in unsaturated soil in a direct shear box set up. The studies conducted include direct shear test on saturated clay sample, soil water characteristic curve, stress-deformation characteristics, percent saturation at various stages of drying on the clay sample.

7.1 Determination of c' and Φ'

The direct shear test was carried out on wet samples (S_r ~ 100%) and the shear strength parameters were determined. The shear strength values were obtained for the respective normal stress values of 20.5 kPa, 52.15 kPa and 90.08 kPa. The wet samples were further allowed saturated for 24 hours. The data points for the time interval of 1 second were monitored using the force transducer. Using the calibration equation, the shear stress exerted on the specimen for the corresponding time was then obtained using the MATLAB code. The horizontal displacement corresponding to the time was obtained by multiplying the strain rate by time. The plot for shear stress vs. the horizontal strain is shown in figure 7.1.

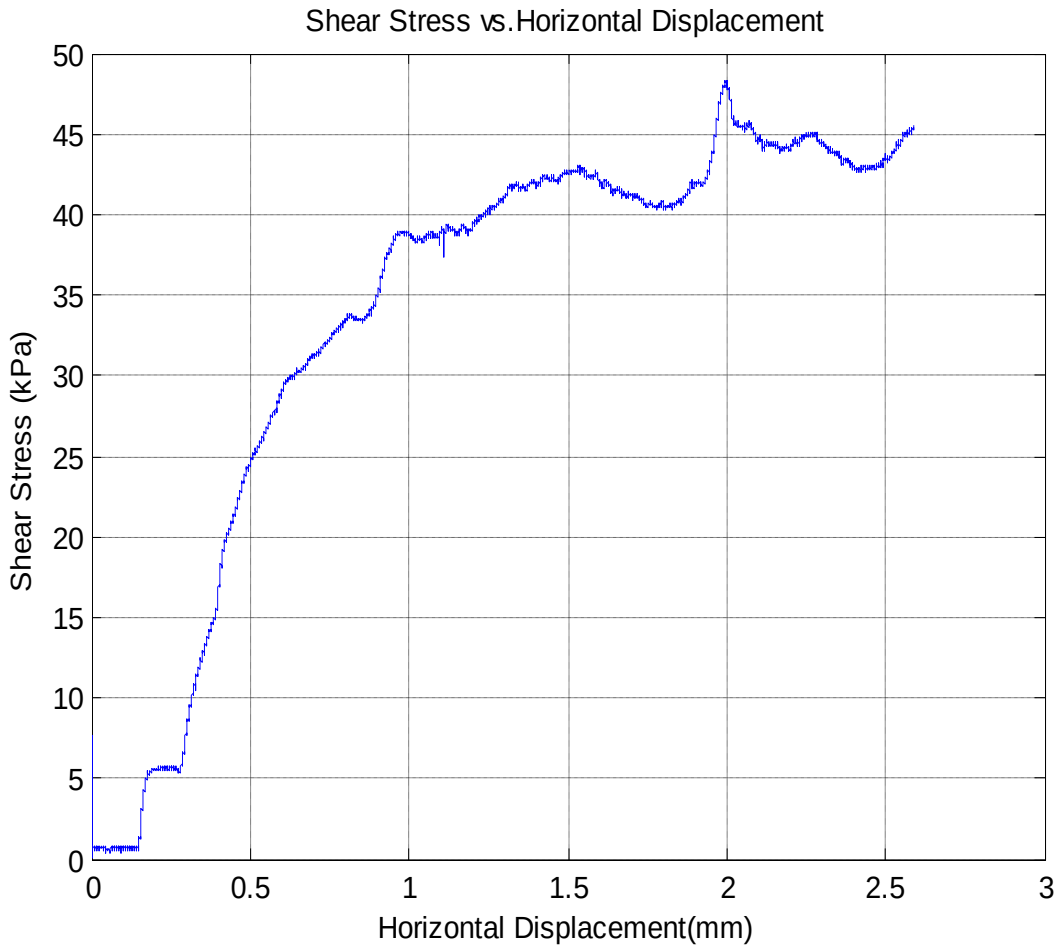

τ	47.5 kPa
σ	90.075 kPa
S_r	92% (~100%)

Fig. 7.1 Plot for shear stress vs. time

Table 7.1 Shear strength values corresponding to the normal stress for saturated soil specimen

Normal load (kg)	Normal stress σ (kPa)	Shear stress τ (kPa)
6.5	20.54	16.45
16.5	52.15	30
28.5	90.08	47.5

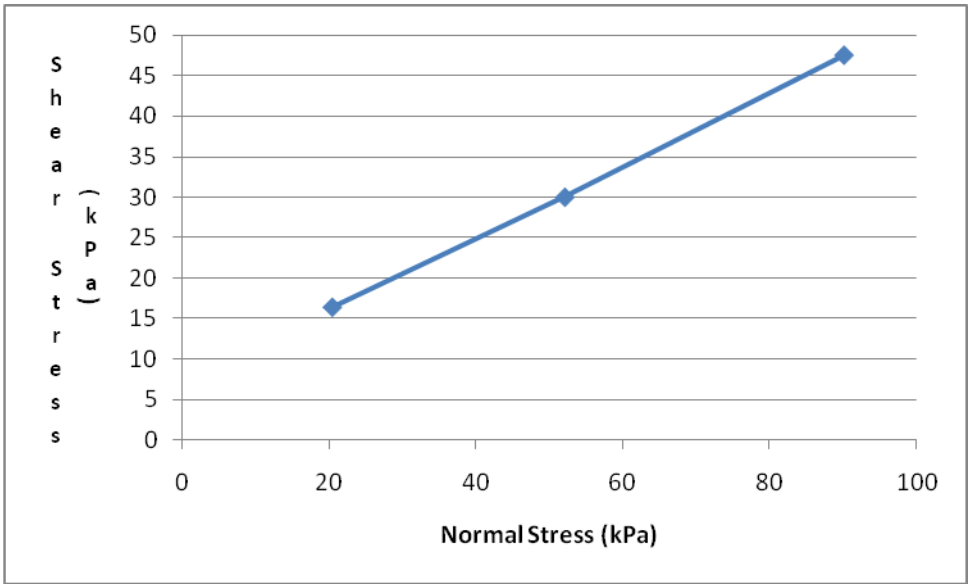

Fig. 7.2 The plot for shear stress vs. effective stress for CD test

Table 7.1 summarizes the test results obtained from the saturated test. The shear stress values obtained from the tests on the saturated samples were plotted against the normal stress as seen in figure 7.2. From the figure 7.2, the friction angle can be measured as:

$\Phi' = 25^0$

For the saturated clay, c' = 0. It was observed that, c' ≠ 0 and this is due to the fact that when the sample was allowed to saturate, only the outer boundary of the sample was saturated and the inner part of the sample remained at its original water content due to the

low permeability value of the sample. The degree of saturation for this inner part was obtained as 92%.

Thus, tensile pore water pressure is exerted on the sample. The field capacity value for the sample is usually observed as 2 pF. The figure 7.2 indicates a field capacity value of 1.995 pF.

7.2 Soil water characteristic curve (SWCC)

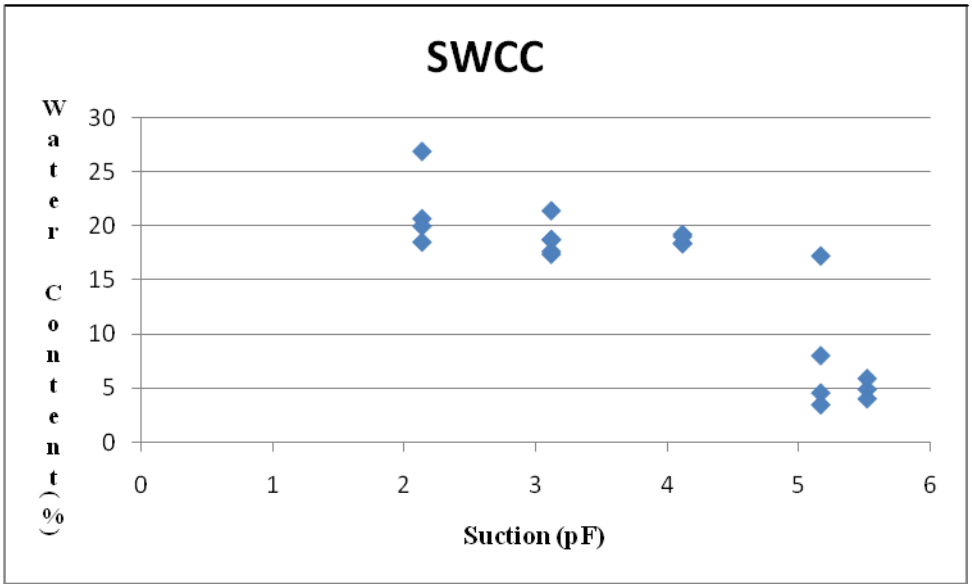

Fig. 7.3 Plot for water content vs. suction from salt equilibrium experiment

The results obtained from the four samples in each jar has been presented in figure 7.3. The soil water characteristic curve as obtained from the salt equilibrium test is presented in figure 7.4.

It can be seen from figure 7.3 that some specimens have not reached equilibrium. These values were ignored and the average water content of the remaining sample points corresponding to a specific suction value was taken. Thus, the values were chosen from this graph and the curve fitting was done to get the equation for the SWCC as shown in figure 7.4

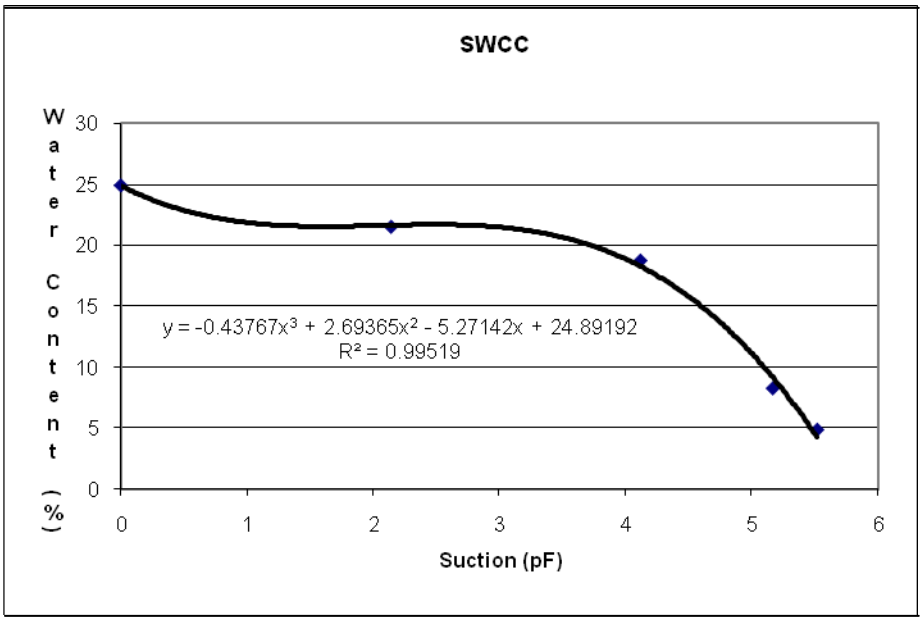

Fig. 7.4 Soil water characteristic curve

7.3 Determination of unsaturated shear strength parameter α for the clay specimen under the study

The direct shear test was conducted on unsaturated dark grey clay specimen. The shear strength for each of these specimens with varying degrees of saturation was obtained from this test. It was observed that the shear strength of the sample increased with the decrease in the water content as seen in Appendix C.

The calculations for effective stress for the sample with S_r = 87.97% is presented next. Figure 7.5 shows the variation of shear stress with horizontal displacement.

τ	124.25 kPa
σ	20.61 kPa
Sr	83.73 %
uw	- 689.76 kPa
α	0.407

Fig. 7.5 Variation of shear stress with horizontal displacement

The shear stress of the sample was measured as 124.25 kPa for a degree of saturation of 83.73% and a normal load of 20.61 kPa. The effective stress for which was determined as:

$$\sigma' = \frac{s}{\tan \Phi'}$$

$$= \frac{124.248}{\tan 25^0}$$

$$= 266.45 \text{ kPa}$$

The water content of the sample on the failure plane was 19.62%. The tensile pore water pressure corresponding to this water content was obtained from the SWCC equation:

$$y = -0.43767x^3 + 2.69365x^2 - 5.27142x + 24.89192 \quad (28)$$

The suction value from this equation was found to be 3.84 pF (= - 689.76 kPa). Now, in the effective stress equation,

$$\sigma = \sigma' + \alpha * u_w + \beta * u_a$$

$$u_a = 0$$

Since, the test was conducted for atmospheric pressure.

Knowing all the parameters, α was back calculated as 0.41 for the sample with degree of saturation equal to 0.84.

7.4 Degree of saturation

The degree of saturation of the sample was obtained by measuring the void ratio for each of the sample. The change in height of the sample during consolidation and shear was monitored and the total volume was calculated. Knowing the dry unit weight and void ratio of the sample, the degree of saturation was calculated. Table D.1 shows the calculations for the degree of saturation.

7.5 Relationship between α and S_r

The data from all the tests for specimens with varying degrees of saturation was analyzed and the plot for α vs. S_r. was obtained as seen in figure 7.5. The best fit curve for the data was obtained and the exponential equation of was formulated for dark grey clay sample with R^2 of 0.81 as seen in equation 30.

$$\alpha = 0.004\, e^{5.5*Sr} \quad (30)$$

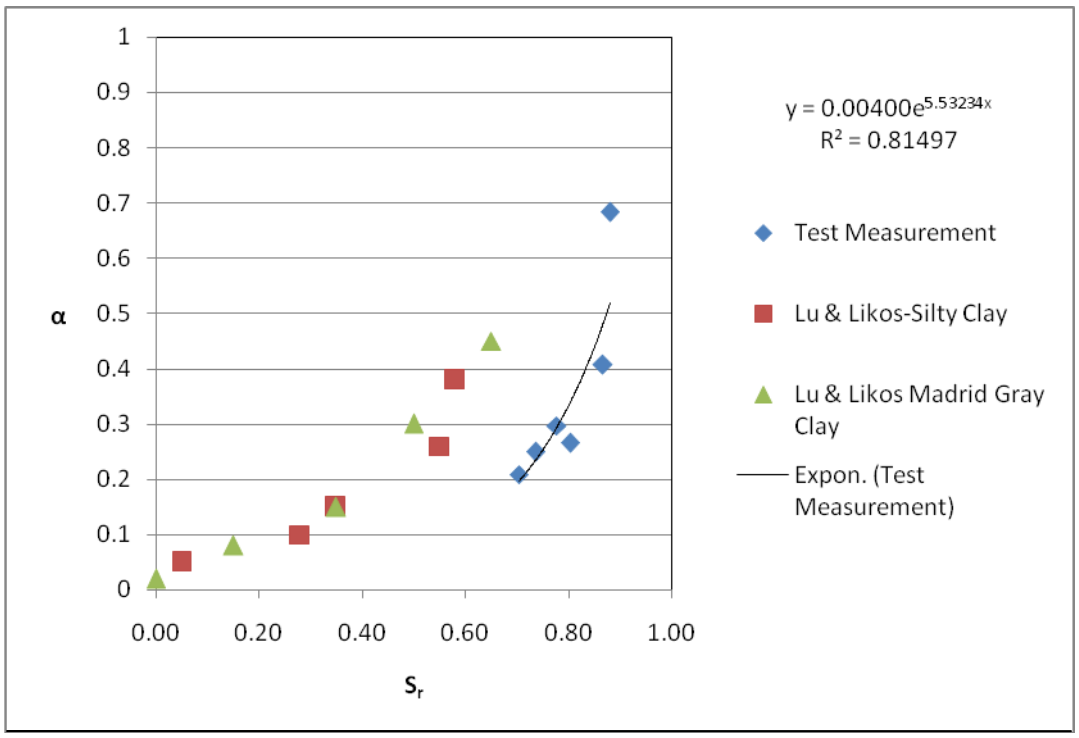

Fig. 7.5 Plot for α vs. S_r

CHAPTER VIII

CONCLUSIONS AND RECOMMENDATIONS

On the grounds of evaluations done in Chapter VII, the conclusions and analysis of this study are summarized as follows.

8.1 Direct shear test on saturated dark grey clay specimen

1. The direct shear test was carried out on the saturated clay specimens for the normal loads of 21.659 kPa, 52.15 kPa and 90.08 kPa. The values of c' and Φ' were measured as 0 kPa and 24^0 respectively.
2. Another important observation from this test was that the field capacity suction of 1.995 pF was observed for the specimen. The field capacity suction of 2 pF is generally considered to be the limiting value. Hence, the measured values of field capacity suction, c' and Φ' are in good agreement with the pertinent information.

8.2 Soil water characteristic curve

1. The soil water characteristic curve was obtained from the salt equilibrium test. It is a low-cost laboratory method and is also used to calibrate other methods. The salt equilibrium test was used since it provides a wider range of suction values.
2. Bulut and Wray (2005) have stated that a period of 14 days equilibrium time is considered to be sufficient. A period of 40 days was allowed for the samples to reach equilibrium to be on the conservative side.
3. It was observed that the SWCC majorly depends on the grain size of the specimen and the hysteresis effect.

4. The SWCC was developed for a range of 0 pF to 5.515 pF corresponding to the gravimetric moisture content of 24.91% to 4.92%. This data has been used to develop the curve.
5. The equation for SWCC (figure 7.4) was obtained as by curve fitting:

   $y = -0.437x^3 + 2.693x^2 - 5.271x + 24.89$

   where,

   y – Gravimetric water content (%)

   x – Suction (pF)
6. This SWCC was used for predicting the tensile pore water pressure of the unsaturated clay specimen.
7. The SWCC was formed by inducing the suction on the inundated specimens such that it results in their drying.

8.3 Unsaturated shear strength test for the clay specimen under the study

Briaud et al. (2007) advocated the effective stress equation as:

$\sigma' = \sigma - \alpha * u_w - \beta * u_a$

All the direct shear tests were carried out on unsaturated clay specimens with varying degrees of saturation for a normal load of 6.5 kg. This normal stress value was chosen in order to accommodate a wider range of degrees of saturation within the instrument range.

The direct shear apparatus was selected for carrying out the shear strength studies owing to the following reasons:

1. The smaller height of the sample allowed quicker drainage. Hence, the time required for consolidation was considerably reduced.
2. The apparatus is simple as compared to triaxial.
3. The cavitation problems are not confronted with by using DST.
4. The failure plane is predetermined. This enables accurate determination of water content of the sample for tensile pore water pressure measurements.
5. The previous literature survey indicated the need for modifying the apparatus in order to apply matric suction on the specimen. The simple

technique was put forth in this research, where the sample was dried outside and thus tensile pore water pressure was induced on the specimen.

6. The weight of the sample was monitored and it was observed that no loss of moisture content occurred while running the test. The humidity level was maintained by keeping a damp cloth on the box. Thus, controlled matric suction conditions were maintained.
7. Holtz and Kovacs (1981) state that the failure for the soil is observed within a range of 15-20% of strain displacement. The previous literature survey indicated that the time to failure for clays is 2-3 days. Hence, a strain rate of 0.00365 mm/min. was chosen for the test. This prohibited generation of excess pore water pressure inside the sample. The failure was assumed when the sample reached the peak and leveled off.

8.4 Degree of saturation for all the unsaturated clay specimens

1. The samples were tested for a range of 87% - 70%. The data is presented in table D.1.
2. Thus, specimens were tested for different tensile pore water pressures.

8.5 Relationship between α and S_r from the clay specimen under the study

The shear strength parameter α significantly depends on:

1. The degree of saturation.
2. The soil structure.
3. The stress history of the soil.
4. The wetting and drying cycles (hysteresis effect).

From all the above parameters, the following equation is established for the clay sample studied:

$$\alpha = 0.004 * e^{5.5*Sr}$$

During this research, it was found that,

$\alpha \neq S_r$

8.6 Future work

The following recommendations are suggested for the future work. It was observed that α is greater than S_r for the sandy and silty soils. For the clayey soils, α is lesser than S_r. The variation of α with S_r might be explained theoretically. The 3D analysis can be presented by zooming at the element level. Figure 8.1 and 8.2 show the representative soil section and view of the soil element with the meniscus respectively. The representative section can be chosen at the centre of the soil grains. Figure 8.3 shows the capillary tension between two soil grains.

The tensile pressure can be defined as:

$$h_c = \frac{2T}{\gamma_w R_s}$$

where,

T = 72 mN/m

The radius of curvature R_s, can be calculated from the known tensile pore water pressure. The water meniscus can be drawn with radius R_s and the centre as shown in the figure.

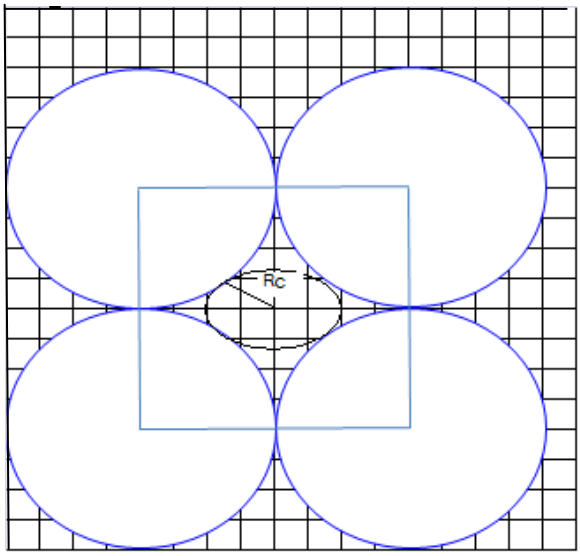

Fig. 8.1 Representative section in the soil system

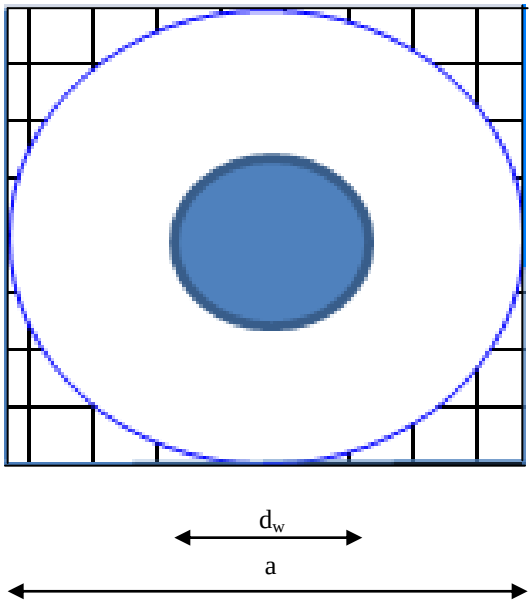

Fig. 8.2 View of the soil grain with the meniscus

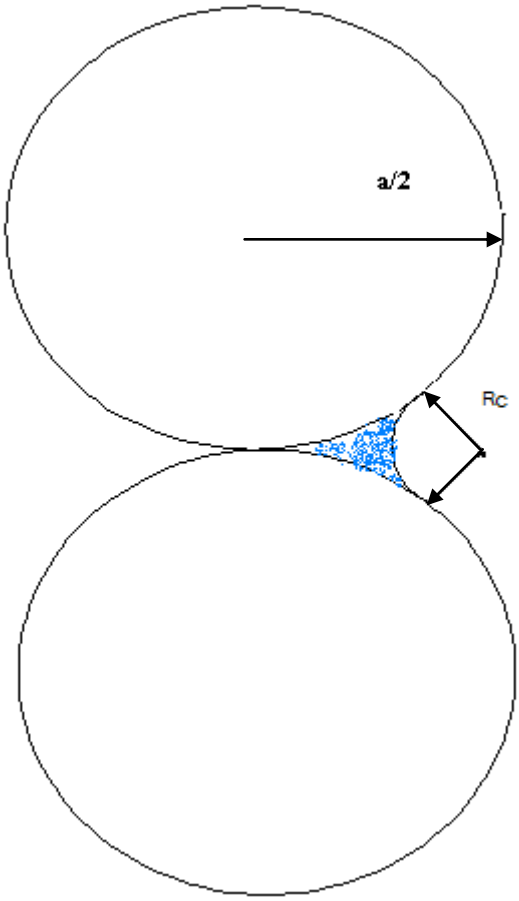

Fig. 8.3 Soil grains and the meniscus

S_r calculations:

Total volume

$V_T = a^3$

Volume of Voids

$$V_V = a^3 - \frac{4}{3}\pi\left(\frac{a}{2}\right)^3$$

α calculations:

Total Area

$A_T = a^2$

Area occupied by water

$$A_w = \frac{\pi}{4} d_w^{\,2}$$

REFERENCES

Ahmed, S., Lowell, C.W. and Diamond, S. (1974). "Pore sizes and shear strength of compacted clay." *ASCE Journal of the Geotechnical Engineering Division*, 100 (GT4), pp. 407-425.

Aitchison, G. D. (1960). "Relationships of moisture stress and effective stress functions in unsaturated soils." *Proc. of the Conference on Pore Pressure and Suction in Soils.* Butterworths, London, UK. pp. 47–52.

Atkinson, John (2000). "Stress in the ground" <http://environment.uwe.ac.uk/geocal/SoilMech/stresses/stresses.htm>

Biscontin, G. (2006). CVEN 649 Class Notes, Texas A&M University, College Station.

Bishop, A.W., and Eldin, A.K.G. (1950). "Undrained triaxial tests on saturated sands and their significance in the general theory of shear strength," *Geotechnique* 2(1).

Bishop, A.W., Alpan, I., Blight, G.E. and Donald, I.B. (1960). "Factors controlling the strength of partly saturated cohesive soils." *Proc. ASCE Res. Conf. on Shear Strength of Cohesive Soils*, Boulder, CO, pp. 503–532.

Blight, G.E. (1961). "Strength and consolidation characteristics of compacted soil." *Ph.D. Dissertation*, University of London, London, England.

Briaud, Jean-Louis, Abdelmalak, R. and Nicks J. (2007) Shrink-Swell Soils Short Course Notes. Texas A&M University, College Station.

Budhu, M. 2000. *Soil Mechanics and Foundations.* John Wiley and Sons.

Bulut, R., Lytton, R. L. and Wray, W. K. (2001). "Soil suction measurements by filter paper." *Proceedings of Geo-Institute Shallow Foundation and Soil Properties*, Geotechnical Special Publication 115, pp 243-261.

Bulut, R. and Wray, W. K. (2005). "Free energy of water-suction-in filter papers." *Geotechnical Testing Journal*, Vol. 28, (4), pp. 355-364.

Campos, T.M.P. and Carrillo, C.W. (1995). "Direct shear testing on an unsaturated soil from Rio de Janerio." *Proc. of 1st International Conf. on Unsaturated soils*, Paris, 1, 31-38

Delage, P. (2002). "Experimental unsaturated soil mechanics." Proc. of 3rd International Conference Unsaturated Soils, 24.

Donald, I.B., (1961). "The mechanical properties of saturated and partly saturated soils with special reference to negative pore water pressure." *Ph.D. Dissertation*, University of London, London, England.

Edil, T.B. (2005). "Shear strength of soils" <http://ecow.engr.wisc.edu/cgi-bin/getbig/cee/730/edil/fall2005le/soilstrength.pdf>

Escario, V. and Saez, J. (1987). "The shear strength of partly saturated soils." *Géotechnique* 36 (3), 453-456

Escario, V. and Juca, J.F.T. (1989). "Strength and deformation of partly saturated soils." *Proc. 12th Int. Conf. on Soil Mechanics and Foundation Engineering*. A. A. Balkema, Bookfield, MA (2), 43-46

Fredlund, D. G., Morgenstern, N. R. and Widger, R. A. (1978). "The shear strength of unsaturated soils." *Canadian Geotechnical Journal,* 15 (3), 313-321

Fredlund, D.G. and Rahardjo, H. (1993). *Soil mechanics for unsaturated soils*, Wiley, New York.

Fredlund, D. G., Xing, A., Fredlund, M.D. and Barbour, S.L. (1995). "The relationship of the unsaturated soil shear strength to the soil water characteristic curve." *Canadian Geotechnical Journal,* Vol. 32, pp. 440-448

Fredlund, D. G. (2006). "Unsaturated soil mechanics in engineering practice." *Journal of Geotechnical and Geoenvironmental Engineering*, pp. 286-321

Gitirana F. N. and Fredlund, D. G. (2004). "Soil-water characteristic curve equation with independent properties" *Journal of Geotechnical and Geoenvironmental Engineering,* 130 (2) pp. 209-212

Herkal, R. N., Vatsala, A. and Murthy, B.R.S. (1995). "Triaxial compression and shear tests on partly saturated soils." *Proc. of the 1st International Conf. on Unsaturated Soils.* Paris, 1, 109-116

Holtz, R. D. and Kovacs, W. D. (1981). *Introduction to Geotechnical Engineering*, Prentice Hall Inc., Englewood Cliffs, NJ

Jennings, J.E. (1960). "A revised Effective Stress Law for Use in the Prediction of the Behavior of Unsaturated Soils." *Proc. of Conf. on Pore Pressure and Suction in Soils*, Butterworths, London, 20-30

Jennings, J.E. and Burland, J.B. (1962). "Limitations to the use of effective stresses in partly saturated soils." *Géotechnique* 12(2), 125-144.

Likos, W. J. and Lu, N. (2002). "Hysteresis of capillary cohesion in unsaturated soils." *15th ASCE Engineering Mechanics Conference*, Columbia University, New York City, NY, 1-8.

Likos, W. J. and Lu, N. (2004). *Unsaturated soil mechanics*, John Wiley and Sons Inc., New Jersey.

Öberg, A. –L. and Sällfors, G. (1995). "A rational approach to the determination of the shear strength parameters of unsaturated soils." *Proc. of the 1st International Conference on Unsaturated Soils*, Paris, 151-157.

Ridley, A.M. and Wray, W.K. (1996). "Suction measurement: A review of current theory and practices." *Proc. of the 1st International Conference on Unsaturated Soils*, Paris, 3, 1293-1322.

Sivakugan, N. (2004). "Effective stress and capillary." <http://www.geoengineer.org/files/siva-effstress.pdf >

Sparks, A.D.W. (1963). "Theoretical considerations of stress equations for partly saturated soils" *Proc. 3rd African Conf. Soil Mech. Found. Engineering.*, Salisbury, Rhodesia, 1, pp. 215-218.

Terzaghi K. (1936). "The shear resistance of saturated soils." *Proc. 1st Int. Conf. Soil Mechanics and Foundation Engineering*, 1, 54-56

APPENDIX A

Data for shear strength of saturated soil

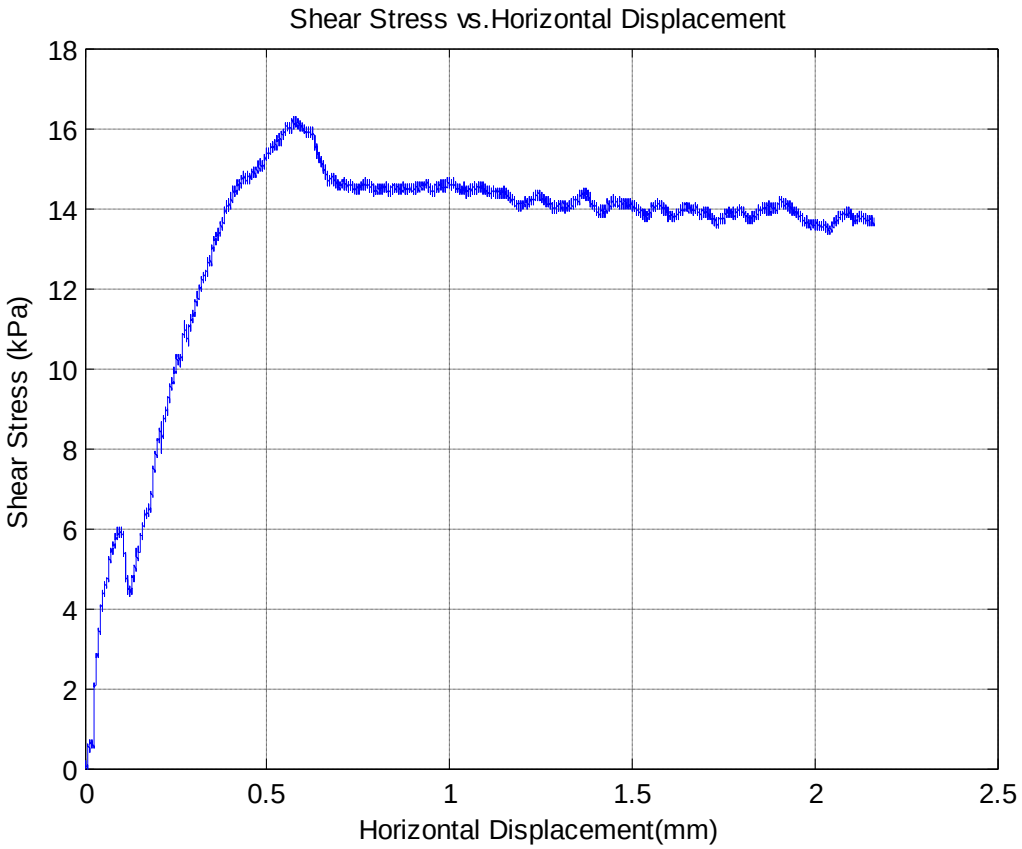

τ	16.452 kPa
σ	20.54 kPa
S_r	92% (~100%)

Fig. A.1 Shear stress vs. horizontal displacement for normal stress of 20.54 kPa

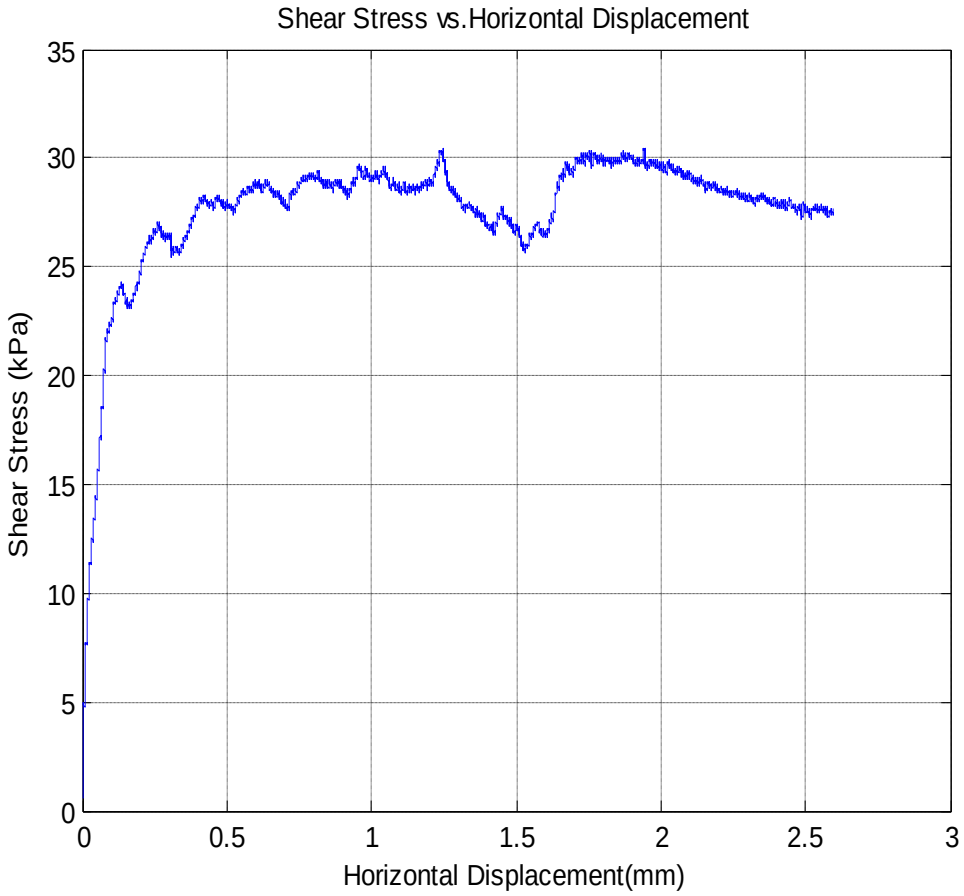

τ	29.925 kPa
σ	52.15 kPa
S_r	92% (~100%)

Fig. A.2 Shear stress vs. horizontal displacement for normal stress of 52.15 kPa

APPENDIX B

Data for shear strength of unsaturated soil

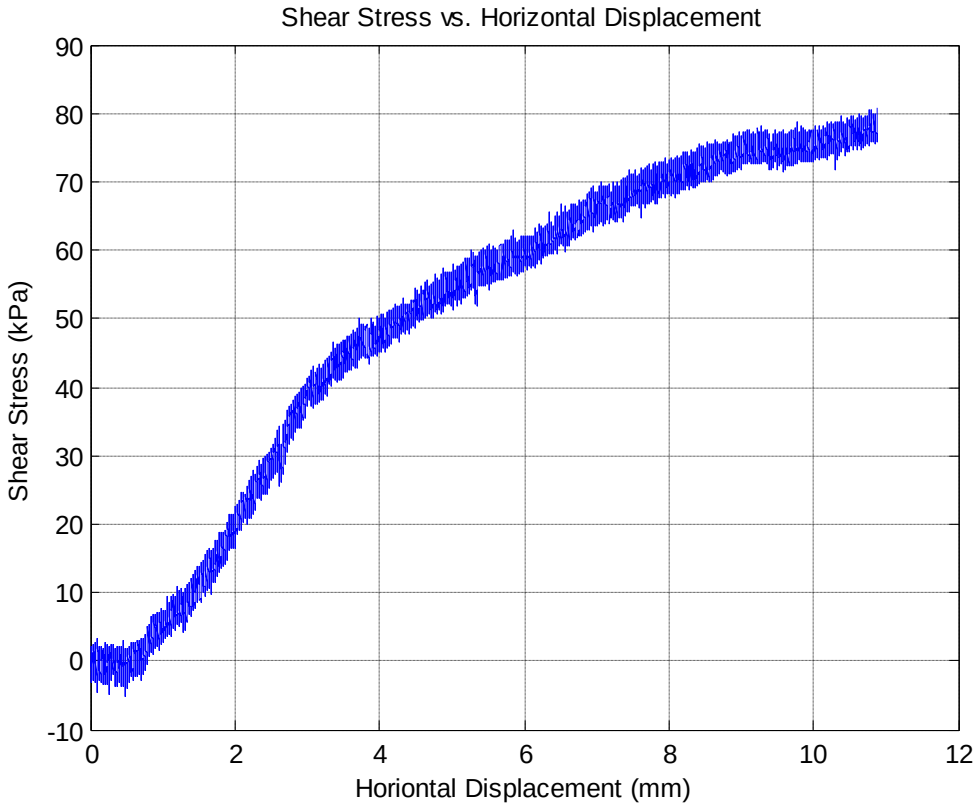

τ	80.71 kPa
σ	21.07 kPa
S_r	87.96%
u_w	-222.68 kPa
α	0.68

Fig. B.1 Shear stress vs. horizontal displacement for S_r of 87.96%

τ	140.52 kPa
σ	22.23 kPa
S_r	80%
u_w	-1051.96 kPa
α	0.27

Fig. B.2 Shear stress vs. horizontal displacement for S_r of 80%

τ	198.012 kPa
σ	21.61 kPa
S_r	78%
u_w	-1357.66 kPa
α	0.297

Fig. B.3 Shear stress vs. horizontal displacement for S_r of 78%

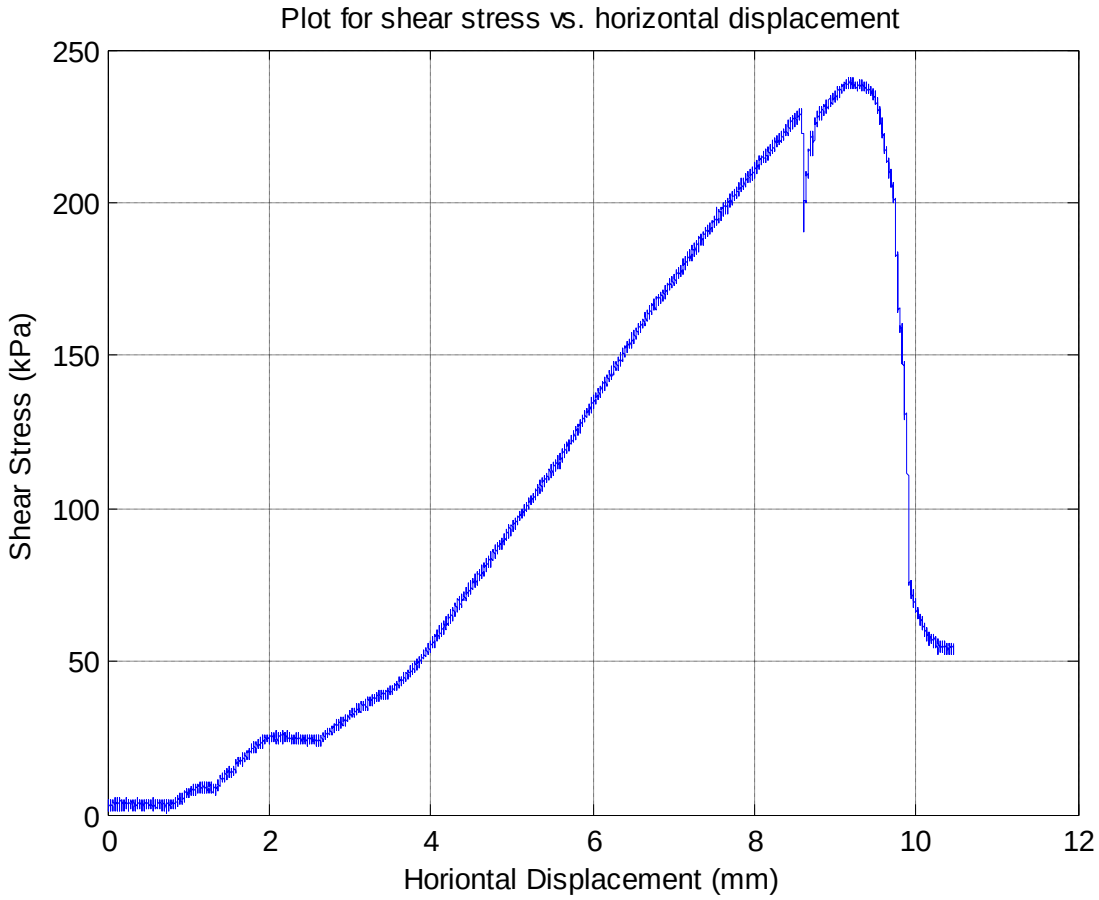

τ	239.03 kPa
σ	21.95 kPa
S_r	74%
u_w	1967.89 kPa
α	0.25

Fig. B.4 Shear stress vs. horizontal displacement for S_r of 74%

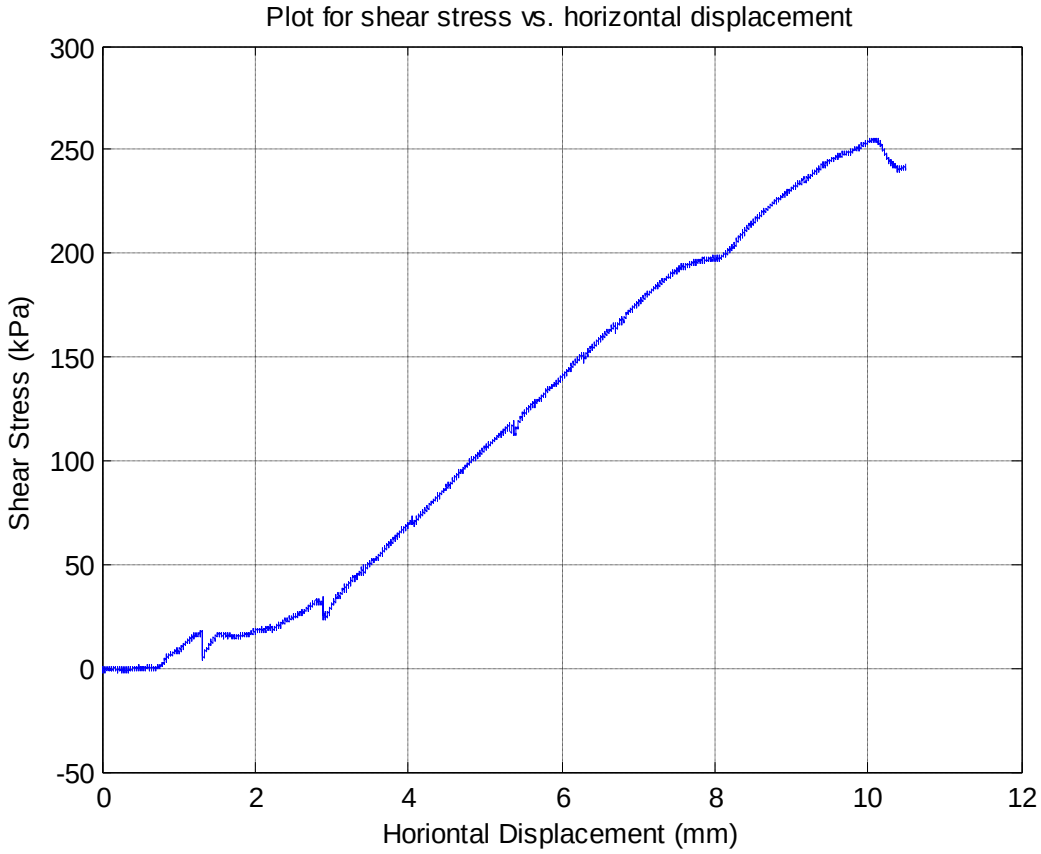

τ	255.64 kPa
σ	21.39 kPa
S_r	70%
u_w	-2522.77 kPa
α	0.21

Fig. B.5 Shear stress vs. horizontal displacement for S_r of 70%

APPENDIX C

Shear Stress vs. Water Content

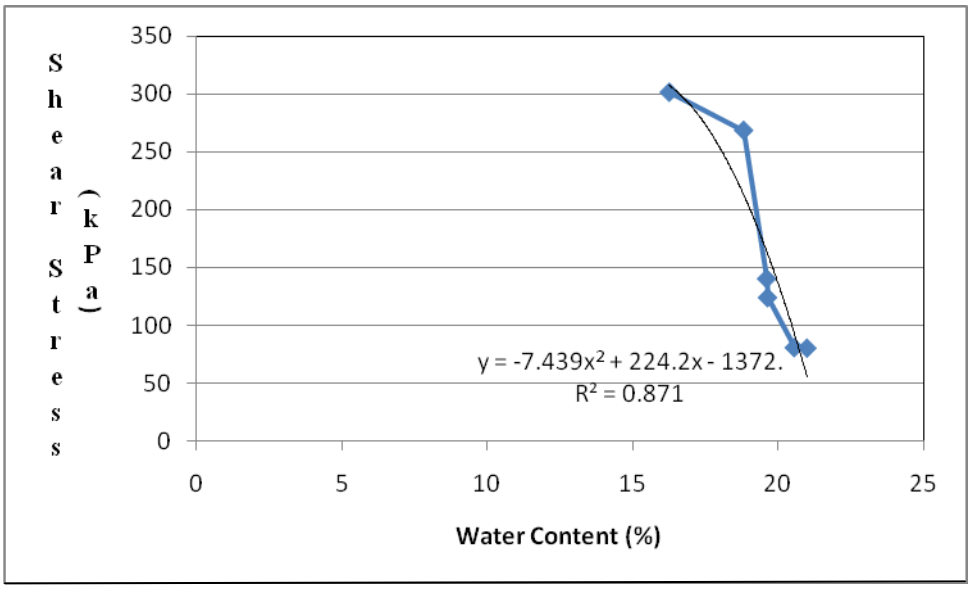

Fig. C.1 Comparison of shear stress vs. water content

APPENDIX D

Data for α and S_r determination

Table D.1 Measurement of degree of saturation

Sample Number	Weight (g)	Height of the sample (mm)	Diameter (mm)	Area (m^2)	Final volume	Total unit weight (kN/m^3)	Water Content (%)	Dry unit weight (kN/m^3)	Void ratio	Degree of saturation (%)
1	156.38	26.42	62.07	0.003026	7.99E-05	19.18964	0.210123	15.85759393	0.6394	0.8796
2	154.22	26.31	61.82	0.003002	7.9E-05	19.15759	0.205709	15.88906979	0.6361	0.8653
3	159.00	26.39	62.77	0.003094	8.17E-05	19.102	0.196204	15.96884403	0.6280	0.8023
4	154.37	26.370	61.81	0.003	7.91E-05	19.14188	0.196523	15.99792394	0.6250	0.7769
5	147.33	26.3	60.43	0.002868	7.54E-05	19.16061	0.188282	16.12463376	0.6122	0.7352
6	143.49	25.8	60.81	0.002905	7.49E-05	18.78431	0.162657	16.15636774	0.6091	0.7036

Table D.2 Presentation of data for determination of α

Sample Number	Time dried (Hours)	Water Content (%)	Shear Stress (kPa)	Diameter of the specimen (mm)	σ (kPa)	σ' (kPa)	S_r	u_w (pF)	u_w (kPa)	α
1	3.23	21.01	80.71	62.07	21.07	173.09	0.88	3.35	-222.68	0.682672
2	5.23	19.62	124.25	62.77	20.61	266.45	0.87	3.84	-689.76	0.406981
3	6.55	18.83	140.52	60.43	22.23	301.33	0.8023	4.022	-1051.96	0.26531
4	6.95	18.26	198.02	61.3	21.61	424.64	0.78	4.14	-1357.66	0.296857
5	8.73	17.31	239.03	60.83	21.95	512.6	0.74	4.3	-1967.886	0.249325
6	8.32	16. 6	255.64	61.602	21.395	548.23	0.704	4.402	-2522.774	0.20883

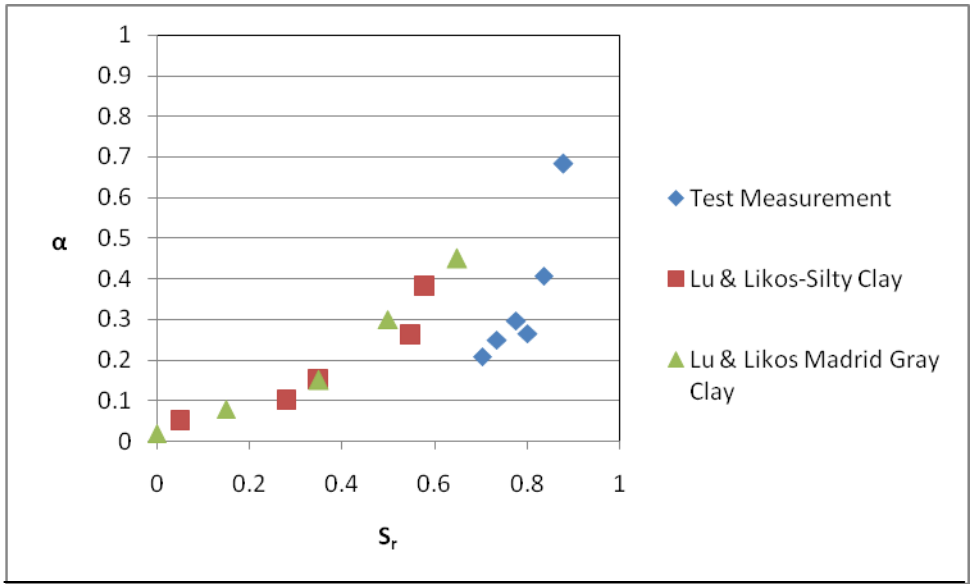

Fig. D.1 Plot for χ vs. S_r for clay specimens

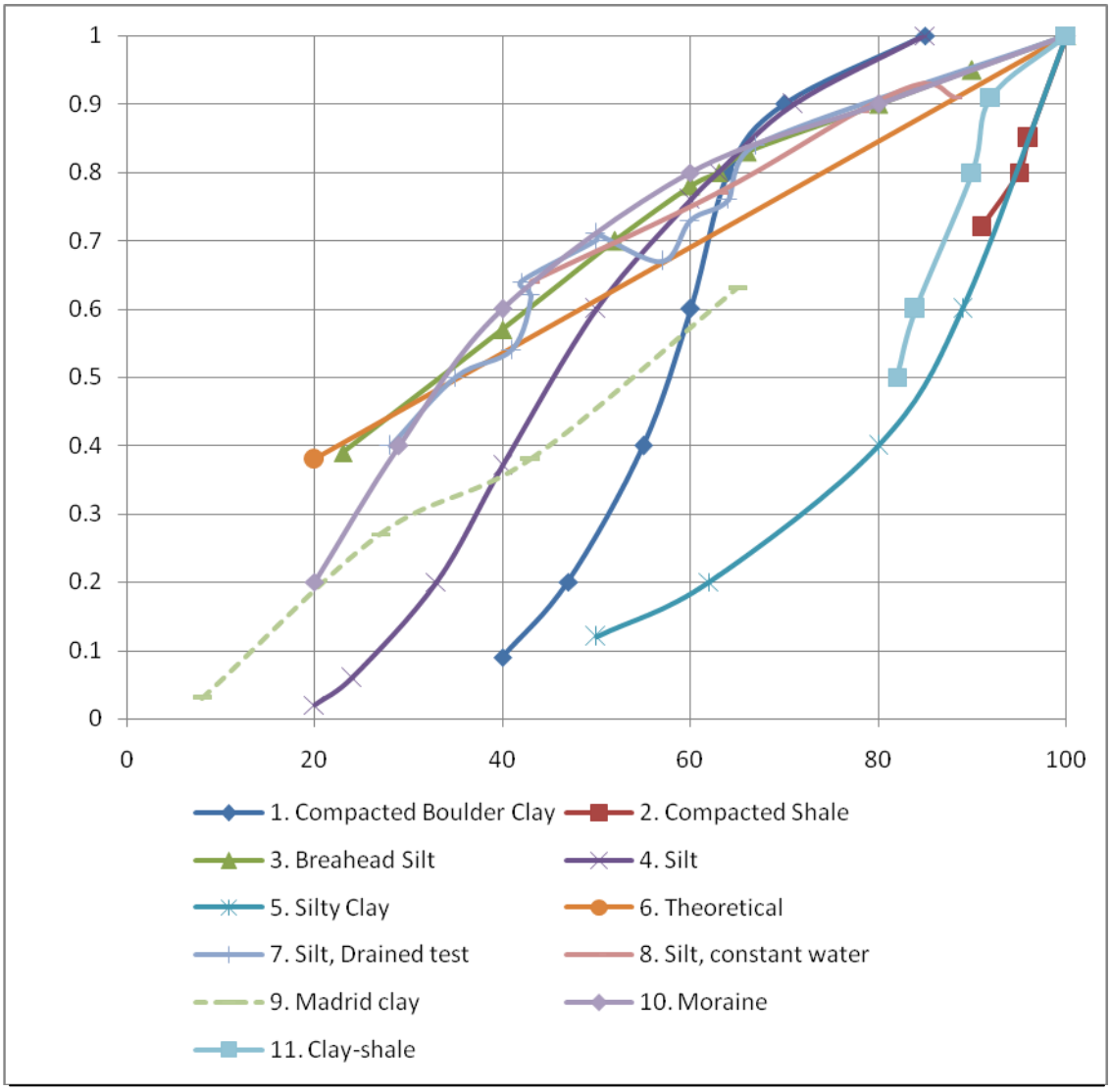

Fig. D.2 Plot for χ vs. S_r for all the specimens

VITA

Name:	Renu Uday Kulkarni
Address:	Texas A&M University, Zachry Department of Civil Engineering, College Station, TX-77843
Email :	renu.uk@gmail.com
Education:	B.E. Civil Engineering, University of Mumbai, Mumbai, India, June 2006 M.S. Civil Engineering, Texas A&M University, College Station, TX-77840, U.S.A., August 2008